

La Physique au Canada

Bulletin de l'Association Canadienne des Physiciens

Physics in Canada

The Bulletin of the Canadian Association of Physicists

Volume 21, No. 2

Congress Issue 1965

Physics in Canada

The Bulletin of the Canadian Association of Physicists

Bulletin de l'Association Canadienne des Physiciens

La Physique au Canada

Vol. 21, No. 2, June 1965

ANNUAL CONGRESS, JUNE 9-12

University of British Columbia, Vancouver, B.C.

Comité d'organisation

Local Committee

Dr. G. M. Volkoff, University of British Columbia
Dr. J. B. Warren, University of British Columbia
Dr. K. C. Mann, University of British Columbia
Dr. R. D. Russell, University of British Columbia
Dr. J. B. Brown, University of British Columbia
Dr. P. J. Sykes, University of British Columbia
Dr. W. V. Olson, University of British Columbia

Comité du Programme

Program Committee

Dr. R. E. Bell, McGill University
Dr. R. W. Stewart, University of British Columbia

C.A.P. EXECUTIVE. *President*: P. Lorrain, University of Montreal. *Past President*: L. Katz, University of Saskatchewan. *Vice-President*: R. E. Bell, McGill University. *Secretary*: A. C. H. Hallett, University of Toronto. *Treasurer*: C. V. Stager, McMaster University. *DIRECTORS*: H. L. Welsh, University of Toronto; C. Fremont, Laval University; Miss M. Hoeksema, University of Western Ontario. *DIVISION CHAIRMEN*: R. A. Beique, Montreal General Hospital, Medical and Biological Physics; E. W. Vogt, Chalk River, Theoretical Physics; J. A. Jacobs, University of British Columbia, Earth Physics. *Registrar*: R. G. Summers-Gill, McMaster University. *Editor*: A. Vallance Jones, University of Saskatchewan.

C.A.P. COUNCIL. *B.C. and Yukon*: R. Barrie, R. M. Pearce. *Alberta*: W. K. Dawson and F. Terentiuk. *Sask. and Man.*: L. H. Greenberg, J. M. Vail. *S.W. Ontario*: P. A. Fraser, L. Krause. *Central Ontario*: J. C. Stryland, Fr. R. Leclaire. *Eastern Ontario*: E. P. Hincks, G. C. Hanna. *Quebec*: P. Marmet, R. Levesque. *New Brunswick and Newfoundland*: S. W. Breckon, A. E. Boone. *Nova Scotia and P.E.I.*: W. J. Archibald, C. R. Mann.

EXECUTIVE ADDRESS: Dept. of Physics, McMaster University, Hamilton, Ont.

PUBLISHED FOR THE ASSOCIATION BY THE UNIVERSITY OF TORONTO PRESS

AUTHORIZED AS SECOND CLASS MAIL BY THE POST OFFICE DEPARTMENT, OTTAWA,
AND FOR PAYMENT OF POSTAGE IN CASH

C.A.P. CONGRESS - 1965 - CONGRES DE L'A.C.P.

PLEASE BRING THIS PROGRAM TO THE CONGRESS
VEUILLEZ APPORTER CE PROGRAMME AU CONGRES

[The meeting of the Royal Society of Canada immediately preceding the C.A.P. Congress includes the following sessions of interest to physicists:

Tuesday, June 8

Location

- | | | |
|-----------|--|-----------------------|
| 9:30 a.m. | Invited papers by three physicists newly elected as Fellows of the Royal Society of Canada (A.V. Jones, J. van Kranendonk, B.P. Stoicheff) | Buchanan 201 |
| 2:00 p.m. | Symposium on Science Education | Frederic Wood Theatre |

Wednesday, June 9

- | | | |
|-----------|---------------------------------|--------------|
| 9:45 a.m. | Symposium on Computer Science] | Buchanan 102 |
|-----------|---------------------------------|--------------|

C.A.P. CONGRESS - 1965 - CONGRES DE L'A.C.P.

The University of British Columbia

June 9 - 12

Vancouver

9 - 12 Juin

ABRIDGED PROGRAM - PROGRAMME ABREGÉ

(the names of invited speakers are given
in brackets - le nom des conférenciers
invités est donné entre parenthèses)

Wednesday, June 9

Location

1:00 - 9:00 p.m.	Registration -- Inscription	Hebb Theatre Lobby
2:00 p.m.	Meeting of Executive and Council	Hennings 301
8:00 p.m.	1. Jointly with the Royal Society of Canada: Symposium on Radio Astronomy (Galt, Walker, Harrower)	Hebb Theatre

Thursday, June 10

8:00 a.m.	Excursion to the Peace River Hydro-Electric Project	Vancouver International Airport
8:30 - 5:30 p.m.	Registration -- Inscription	Hebb Theatre Lobby
9:00 a.m.	2. Symposium on Polarized Beams and Targets (Jeffries, Craddock, Hird, Gerhart, Vogt)	Hebb Theatre
9:00 a.m.	3. Symposium on Isotope Geophysics (Richards, Reynolds)	Hennings 202
9:00 a.m.	4. Solid State Physics	Hebb 10
9:00 a.m.	5. Experimental Nuclear Physics I	Hennings 201

1:45 p.m.	Presidential Address and business meeting (N.B. starts at 1:45 p.m.)	
	Discours du président et réunion plénière (N.B. commence à 1:45 hre.)	Hebb Theatre
4:30 p.m.	Visit to Simon Fraser University	Hebb Theatre Steps
8:30 p.m.	Musical Evening	Hebb Theatre

Friday, June 11

9:00 a.m.	6. Symposium on Crustal Structures in Canada	Hebb 10
9:00 a.m.	7. Canadian Physics (Whitehead, Bartholomew)	Hennings 202
9:00 a.m.	8. Upper Atmospheric Physics	Hebb 13
9:00 a.m.	9. Apparatus of Nuclear Physics	Hennings 201
2:00 p.m.	10. Astronomy (Moffatt, Cummings)	Hennings 202
2:00 p.m.	11. Theoretical Symposium (McMillan, Tabakin, Schwartz, Christy)	Hebb 10
2:00 p.m.	12. Experimental Nuclear Physics II	Hennings 201
2:00 p.m.	13. Atomic and Molecular Physics	Hebb 13
6:00 p.m.	Pre-dinner social hour	Brock Hall
7:00 p.m.	Banquet of the C.A.P. Presentation of the C.A.P. Prize. Presentation of the C.A.P. Medal to H.E. Johns. After-dinner speaker: the Hon. Leslie R. Peterson, Minister of Education and Labour of British Columbia.	Brock Hall

Saturday, June 12

- | | | |
|------------|---|--------------------|
| 9:00 a.m. | 14. Onium (Positr- and Mu-) and
Mu-Mesic Atoms (Rothberg,
Jones, Hincks) | Hennings 201 |
| 9:00 a.m. | 15. Plasma Physics (Thompson) | Hennings 202 |
| 9:00 a.m. | 16. Theoretical Topics | Hebb 10 |
| 12:00 noon | Trip to Vancouver Island | Hebb Theatre Steps |
| 2:00 p.m. | Joint meeting of the old
and new Councils | Hennings 303 |

C.A.P. CONGRESS - 1965 - CONGRES DE L'A.C.P.

PROGRAM - PROGRAMME

Wednesday, June 9, 1:00 - 9:00 p.m. Hebb Theatre Lobby

Registration - Inscription

Wednesday, June 9, 2:00 p.m. Hennings 301

Meeting of Executive and Council

Wednesday, June 9, 8:00 p.m. Hebb Theatre

Session 1. Joint Symposium: RADIO ASTRONOMY
(with the Royal Society of Canada)
Chairman: G.M. Volkoff Convener: F.T. Davies

- 1.1 LOW FREQUENCY RADIO ASTRONOMY (30 min.)
J.A. Galt and C.R. Costain, Radio Astrophysical Observatory,
Penticton (To be delivered by Dr. Galt.)
- 1.2 OPTICAL ASTRONOMICAL OBSERVATIONS RELATED TO RADIO ASTRONOMY
(30 min.)
G.A.H. Walker, Dominion Astrophysical Observatory, Victoria.
- 1.3 RADIO ASTRONOMY AS A TOOL IN COSMOLOGICAL RESEARCH (30 min.)
G.A. Harrower, Queen's University.

Thursday, June 10, 9:00 a.m. Hebb Theatre

Session 2. Symposium on POLARIZED BEAMS AND TARGETS

Chairman: J.B. Warren

- 2.1 POLARIZED TARGETS (30 min.)
C.D. Jeffries, University of California, Berkeley.
- 2.2 POLARIZED ION SOURCES AND BEAMS (30 min.)
M.K. Craddock, University of British Columbia.
- 2.3 PLANS FOR POLARIZED PROTONS FROM THE MANITOBA CYCLOTRON (30 min.)
B. Hird, University of Manitoba.
- 2.4 SPIN-FLIP REACTIONS (30 min.)
James B. Gerhart, University of Washington, Seattle.
- 2.5 NUCLEAR REACTIONS WITH POLARIZED PARTICLES (30 min.)
E.W. Vogt, University of British Columbia.

Session 3. Symposium on ISOTOPE GEOPHYSICS

Chairman: R.D. Russell

3.1 GEOCHRONOLOGY AND LEAD ISOTOPE GEOLOGY AT MOUNT ISA, AUSTRALIA (30 min.)

J.R. Richards, Department of Geophysics and Geochemistry, Australian National University, Canberra.

This address is intended as a progress report on the study of the time relationship between mineralisation and tectonic activity in what appears to be a reasonably well-authenticated stratiform sulphide deposit of major proportions. Granitic rocks in the surrounding regions have been analysed for K/Ar ratio in micas, Rb/Sr ratio in micas and whole-rock samples, and Pb/U-Th ratios in some zircon concentrates. Relative abundances of lead isotopes have been made for two stratiform deposits in this region. Some discussion will be made of the implication of the results as they now stand, and of the future steps envisaged.

3.2 ZENOLOGY (30 min.)

J. Reynolds, University of California, Berkeley.

3.3 THE U.B.C. POTASSIUM-ARGON DATING LABORATORY

G.P. Erickson and M.J. Harakal, Department of Geophysics, University of British Columbia.

The potassium-argon dating laboratory at U.B.C. has now been in operation for more than a year. This paper is a report on the unusual features of design and application of the analytical equipment in the laboratory. These include the statically operated AEIMS10 mass spectrometer and its modifications, the ultra-high vacuum system utilizing an ion pump, the Ar³⁰ spike and atmospheric argon metering systems, and the Baird-Atomic KY1 flame photometer. Analytical data and their geological implications are being presented in detail elsewhere and will be summarized here.

3.4 LEAD ISOTOPE RELATIONSHIPS OF GRANITES, VOLCANICS, AND SULFIDE ORES ASSOCIATED WITH THE BOULDER BATHOLITH, MONTANA

Bruce R. Doe and Maryse H. Delevaux, U.S. Geological Survey, Denver, Colorado.

3.5 A METHOD OF RATIO RECORDING FOR LEAD ISOTOPES IN MASS SPECTROMETRY

John S. Stacey, U.S. Geological Survey, Denver, Colorado.

3.6 SULPHUR ISOTOPE VARIATIONS IN CO-EXISTENT SULPHIDES IN THE QUEMONT MINE

G. Ryznar, F.A. Campbell, Department of Geology, H.R. Krouse, Department of Physics, University of Alberta, Edmonton.

A detailed study has been made of the S^{34}/S^{32} variations of a large number of samples of co-existing pyrite, pyrrhotite, sphalerite and chalcopyrite taken from various depths down to 3000 feet from the Quemont mine. Most of these sulphides had S^{34}/S^{32} ratios within the narrow range of 0 to + 2 * δ - units with respect to a meteoritic troilite reference. Between the 900 and 3100 foot levels, the pyrites showed a consistent increase in S^{34} content with depth which was less than 1 δ unit for the entire range. Sphalerites and chalcopyrites were generally depleted in S^{34} with respect to the pyrites. Possible interpretations of these results will be presented.

$$* \delta_{34} = \frac{S^{34}/S^{32} \text{ sample}}{S^{34}/S^{32} \text{ meteorite}} - 1 \quad \times 1000$$

3.7 S^{34}/S^{32} VARIATIONS IN SOME LOW TEMPERATURE LEAD-ZINC DEPOSITS OF WESTERN CANADA

T.L. Evans, F.A. Campbell, Department of Geology, and H.R. Krouse, Department of Physics, University of Alberta, Edmonton.

A reconnaissance study was made of S^{32}/S^{34} ratios in 31 sulphide samples from Kicking Horse, Monarch, Hawk Creek, Eldon, Baker Creek, Beaver River, and Pine Point deposits. All of these samples were enriched by 8 to 31 δ -units* in S^{34} with respect to a meteorite troilite standard, the average being +19 δ -units. Pyrite was found to be enriched in S^{34} by as much as 3 δ -units with respect to co-existing sphalerite. In 6 out of 8 cases, the sphalerite was found to be enriched in S^{34} by as much as 5 δ -units with respect to co-existing galena. These observations suggest the order of deposition; pyrite, sphalerite and galena from a sulphur reservoir becoming enriched in S^{32} .

$$* \delta_{34} = \left(\frac{S^{34}/S^{32} \text{ sample}}{S^{34}/S^{32} \text{ meteorite}} - 1 \right) \times 1000$$

3.8 VARIATIONS IN THE O^{18}/O^{16} RATIO IN ICE AND SNOW FROM THE HUBBARD AND KASKAWULSH GLACIERS IN THE ST. ELIAS MOUNTAINS

D.S. MacPherson, Department of Geology, and H.R. Krouse, Department of Physics, University of Alberta, Edmonton.

One hundred samples for this study were taken during the summer of 1963 from the Hubbard and Kaskawulsh glacier systems with the idea of (i) co-relating O^{18}/O^{16} variations with annual meteorological trends and (ii) using the O^{18}/O^{16} ratio as a natural tracer of glacier flow. The δ -values* found for snow and ice ranged from -17.7 to -29.2 with respect to standard

mean ocean water (SMOW). These variations compare favorably with the work of Epstein et al¹⁾ on the Malispina glacier in the same general area. A definite co-relation exists between snow samples from pit studies on the Kaskawulsh glacier and the glaciology and the annual precipitation pattern of the area. It has been demonstrated that subsequent downward percolation of summer melt water produced a homogenization of the O^{18}/O^{16} ratio diluting the significant annual pattern noticed prior to the summer melt season. An altitude effect was noticed in the hard ice below the fern line that tends to support existing theories as to the mode of glacier flow.

$$* \delta_{18} = \left(\frac{O^{18}/O^{16} \text{ sample}}{O^{18}/O^{16} \text{ SMOW}} - 1 \right) \times 1000$$

- 1) S. Epstein and R.P. Sharp, Oxygen Isotope Variations in the Malispina and Saskatchewan Glaciers. *J. Geol.* **67**, 88-102 (1959).

3.9 A TELLURIUM ISOTOPE FRACTIONATION STUDY

R.M. Smithers and H.R. Krouse, Department of Physics, University of Alberta, Edmonton.

Theoretical calculations have been made which suggest that the Te^{122}/Te^{130} ratio may be altered by over 2 percent in laboratory reactions and natural processes. A preliminary study has realized variations of as high as 0.7 percent in the Te^{122}/Te^{130} ratio in chemical and microbiological reduction studies in the laboratory. One natural sample has been found to be 0.4 percent enriched in the lighter isotope in comparison with others which have a fairly constant ratio. These results will be discussed in comparison to similar results found for selenium and sulphur isotopes.

3.10 THE OBSERVATION OF EXCESS AMOUNTS OF RADIOGENIC ARGON IN FELSPATHOID MINERALS

Derek York and R.M. Macintyre, Department of Physics and J. Gittins, Department of Geology, University of Toronto.

The feldspathoid minerals cancrinite and sodalite have been found to contain excessive quantities of radiogenic argon. The excess amount of Ar^{40} is of the order 10^{-4} cc. n.t.p./gm in cancrinite and ranges from 10^{-6} - 10^{-5} cc.n.t.p./gm in sodalite. Another feldspathoid, nepheline, does not appear to contain excess Ar^{40} and actually seems to be a reliable indicator of geological age. The origin of excessive amounts of argon in crystals will be discussed in relation to these observations. Argon volumes were measured by the isotope dilution method and potassium concentrations were determined by flame photometry.

3.11 LEAD ISOTOPE RATIOS IN VOLCANIC ROCKS

M. Tatsumoto, U.S. Geological Survey, Denver, Colorado.

Session 4. SOLID STATE PHYSICS

Chairman: R.R. Haering

4.1 PROPERTIES OF SILVER OXIDE FILMS

T.L. Rollins and F.L. Weichman, University of Alberta, Edmonton

Thin films of silver oxide were deposited by cathodic sputtering of silver in oxygen atmosphere as previously described 1) on a mica substrate held at approximately -100°C . The samples obtained were initially of low resistance (10^5 ohms), opaque in the visible region and non-photoconducting. The material was found to be unstable. Over period of weeks the resistance steadily increased and at the same time the material became photoconducting. These reproducible changes could be accelerated by heating the samples in air to up to 100°C . Too high a temperature caused decomposition of the oxide into silver. The energy gap as obtained from optical transmission, electrical conductivity and/or photoconductivity measurements was found to increase from about 0.9 eV for fresh samples to about 1.5 eV after the changes had taken place. Final resistance of the samples amounted to about 10^{11} ohms.

1) E. Fortin and F.L. Weichman, phys. stat. sol. 5, 519 (1964)

4.2 "IN-BAND" MODES OF VIBRATION OF A DILUTE DISORDERED ALLOY - Cu(Au).

E.C. Svensson, B.N. Brockhouse and J.M. Rowe, McMaster University.

Using neutron scattering, we have studied the lattice vibrations of a single crystal, containing 9.3 atomic percent gold as a substitutional impurity in a copper host lattice. The [100] transverse branch was studied in detail; the [111] transverse zone-boundary phonon was also measured. A comparison is made with the corresponding vibrations in pure copper. The measurements were carried out using the Chalk River triple-axis spectrometer in the "Constant-Q" mode of operation. The Cu(Au) phonons are asymmetric and broader than the corresponding copper phonons; they are also lower in frequency. The results are somewhat reminiscent of those predicted by the theory of Elliott and Maradudin¹⁾ which considers mass changes only and which is strictly valid only in the limit of small defect concentration. However, serious discrepancies are observed.

1) R.J. Elliott and A.A. Maradudin, I.A.E.A. Conference on Inelastic Scattering of Neutrons in Solids and Liquids, Bombay, India, Dec. 1964, (to be published).

4.3 THERMAL PULSES IN SAPPHIRE

J.B. Brown and D.Y. Chung, Department of Physics, University of British Columbia.

Ward and Wilks¹⁾ suggested that Landau's description of liquid helium implied that the phenomenon of second sound, or thermal propagation obeying a wave rather than diffusion equation, might occur in solids. It can be distinguished from ordinary acoustic propagation by having a mean free path for normal phonon collisions much shorter than a wavelength, thus being pictured as a density wave propagated in the phonon gas. Artificial sapphire exhibits an unusually high thermal conductivity and seems one of the most promising solids to investigate. The difficulty of obtaining a sensitive thermal detector with a microsecond response time between 4°K and 40°K has been met by the use of a thin film of indium placed in the coil of a radio frequency bridge. The character of the propagation can be conveniently analysed in terms of the analogous electrical transmission line, the assumption of simple diffusion in a solid being equivalent to neglecting an inductive term representing thermal inertia. This analysis of the results and the variation of propagation velocity with temperature will be discussed.

1) J.C. Ward and J. Wilks, *Phil. Mag.* 45, 48 (1952).

4.4 WORK FUNCTION OF TUNGSTEN SINGLE CRYSTALS

H.M. Love and J.R. Wilson, ^{*} Department of Physics, Queen's University.

Measurements have been made of the work functions of tungsten crystals in an ultra-high vacuum system by a method previously reported¹⁾.

The work function of a tungsten single crystal with the (311) plane 5 degrees from the surface was found to be 4.15 ± 0.07 volt. The value for a single crystal with the (310) plane within one degree of the surface was $4.31 \pm .07$ volt.

The method used in this work gives differences between the work functions of two surfaces more precisely than the value of either, this difference for the two surfaces mentioned above being 162 ± 2 millivolt. The value obtained for the Richardson constant was $1.05 \times 10^5 \pm .49 \times 10^5$ a.m.⁻². (°K)⁻².

* Now with Department of Mines & Technical Surveys, Division of Oceanographic Research.

1) H.M. Love and G.L. Dyer, *Can. J. Phys.* 40, 1837 (1962)

4.5 THERMAL CONDUCTIVITY OF POTASSIUM - CESIUM ALLOYS

M. Archibald, J. Dunick and M.H. Jericho, Physics Department, Dalhousie University.

We have measured the electrical and thermal conductivity of potassium base alloys containing up to 10 At% cesium in solid solution. The measurements were made between 4.2°K and 1.8°K.

In this temperature range the total thermal conductivity

for most samples can be represented by the equation

$$\kappa = \frac{L_0 T}{C_0} + \frac{B}{C_0} T^n$$

where n is approximately 1. Two samples were measured down to 0.4°K and around 0.5°K the thermal conductivity is given by the Wiedemann-Franz law to within the experimental error. The lattice thermal conductivities calculated from the measured total conductivities are much smaller than those predicted by simple theories that consider phonon-electron scattering only.

4.6 HALL EFFECT AND ELECTRICAL CONDUCTIVITY OF Cu_2O

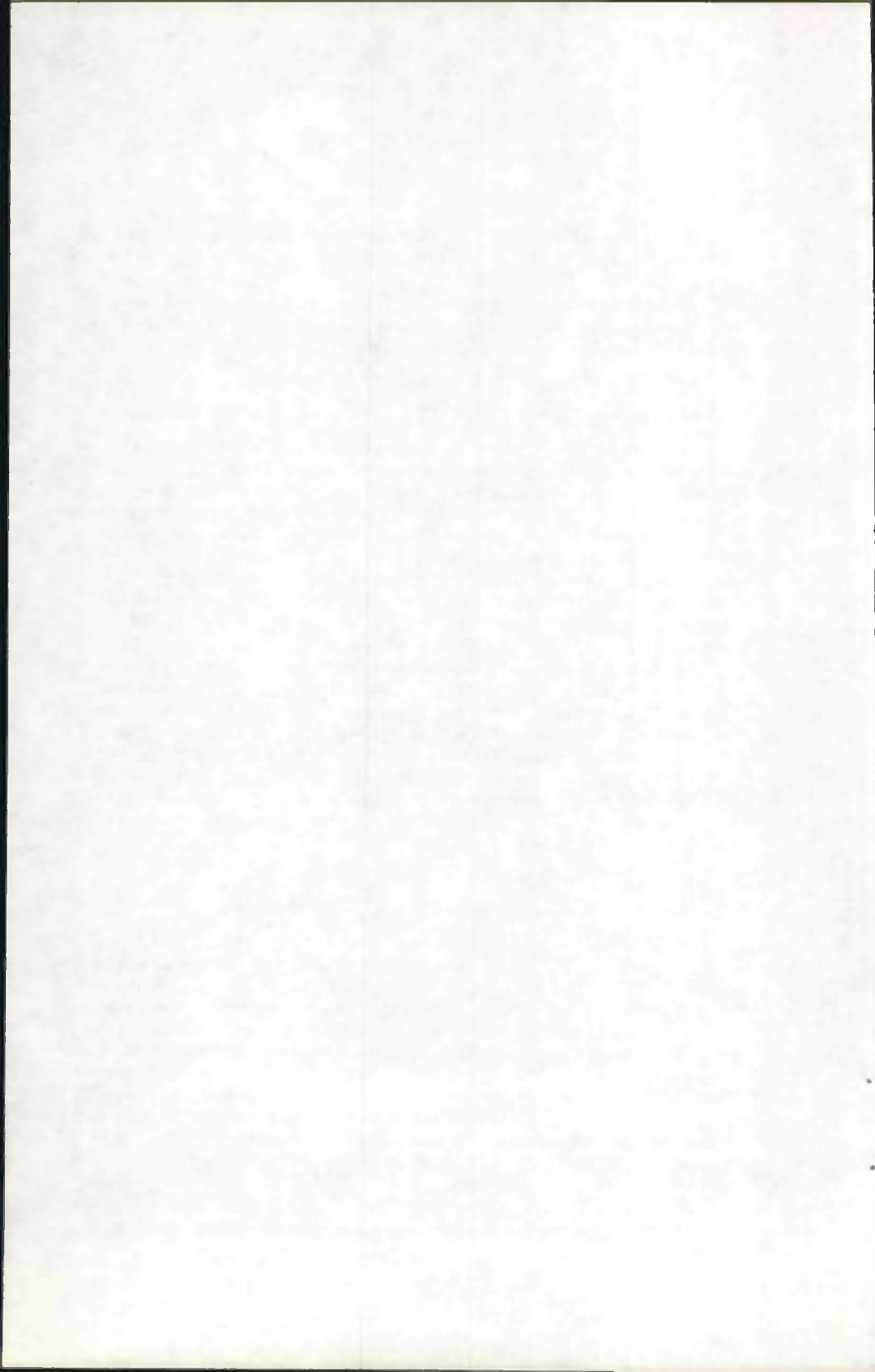
E. Fortin and F.L. Weichman, University of Alberta, Edmonton.

Hall effect and electrical conductivity measurements were performed on different Cu_2O samples from polycrystalline to single crystals. Measurement below and above room temperature were taken both before and after annealing the samples in vacuo at temperatures ranging from 200 to 1000°C. Both the absolute values of mobility and conductivity as well as their temperature dependence were found to be strongly altered by the annealing process. Room temperature conductivities usually dropped from 10^{-6} to $10^{-8} \Omega^{-1} \text{cm}^{-1}$ while the mobility increased from 10 - 30 to 120 $\text{cm}^2/\text{V-sec}$ after annealing. Similarly, the conductivity slopes were higher and regions of exponential temperature dependence for the mobility showed up. Reproducibility within a sample as well as for different samples could be obtained only after annealing the specimens. The mobility is also found to be independent of the electric and magnetic fields in the 0-2 KV/cm, 0-16 KG ranges. The results are compared to previous investigations and it is shown that the wide variety in data could be due to various thermal histories of different samples.

4.7 QUANTUM THEORY OF HELICONS

P.R. Wallace, McGill University.

The calculation of the dispersion relation for collective modes of excitation of electrons in solids may be deduced from a calculation of the frequency - and wavelength - dependent conductivity tensor. Making use of the calculation of this tensor for free electrons in a magnetic field by Quinn and Rodriguez (Physical Review, 128, 2487, (1962)), a quantum theory of helicons is derived in this case. This may then be extended to other types of energy surface in solids, including the case of multiple surfaces. Circumstances which lead to the presence of more than one branch to the excitation spectrum will be discussed.



4.10 THE INELASTIC REFLECTION OF SLOW ELECTRONS FROM SINGLE CRYSTALS OF TUNGSTEN

R.A. Armstrong, Radio and Electrical Engineering Division, National Research Council of Canada, Ottawa.

The inelastic reflection of electrons from clean W(100) and W(211) crystal surfaces has been studied. For energies less than about 4 eV no inelastically reflected electrons are observed. A sharp threshold for inelastic production is found at about this energy. Additional rapid increases in the number of electrons reflected inelastically are found at higher energy. These results will be compared with the measurements of elastic reflection from the same surfaces.

4.11 THE CONDUCTION BAND OF GaSb

J.C. Woolley and H.B. Harland, Department of Physics, University of Ottawa.

Measurements of Hall coefficient and magnetoresistance have been made on various samples of single crystal tellurium-doped GaSb in the temperature range 1.8°K to room temperature and with magnetic fields up to 24 Kgauss. A two band analysis of these results plus assumptions concerning scattering mechanisms provide values of carrier concentrations n_0 and n_1 and electron drift mobilities μ_0 and μ_1 in the (000) and <111> conduction band minima respectively. The variation of n_0 and n_1 with temperature enable values to be determined for the effective mass of electrons in the <111> minima (m_1^*), the energy separation of the (000) and <111> minima (ΔE) at absolute zero and the temperature coefficient of ΔE . The values obtained for these parameters are:

$$m_1^* = 0.49 m_e \qquad \Delta E_0 = 0.084 \text{ eV}$$

$$\frac{d}{dT}(\Delta E) = +7.2 \times 10^{-5} \text{ eV/}^\circ\text{K.}$$

The mobility ratio $\frac{\mu_0}{\mu_1}$ is found to take values in the range 6-30 for various conditions of carrier concentration and temperature. An important factor in this variation is the large increase in μ_0 when conditions allow the <111> minima to be populated.

4.12 SPIN-LATTICE RELAXATION TIMES AND THE PHASE TRANSITIONS IN METHANE

G.A. de Wit, Department of Physics, University of British Columbia.

Measurements of proton and deuteron spin-lattice relaxation times in purified CD₃H and CH₄ were carried out from 1.3°K to 55°K, using the spin-echo technique of nuclear magnetic resonance, to obtain more information about the phase transitions in methane

and its isotopic modifications. In the case of CD_3H , the proton spin-lattice relaxation time is essentially constant from 550K down to the phase transition temperature (25.50K), below which it decreases very strongly and goes through a minimum. The deuteron spin-lattice relaxation time exhibits identical features, but the change in T_1 is larger than for the proton spin-lattice relaxation time. The proton spin-lattice relaxation time in CH_4 is a constant down to 20°K (the transition temperature), below the transition temperature there is a large change in the relaxation time and it becomes essentially a constant below 10°K.

All of these results show there is large change in the rotational degree of freedom of the molecule at the upper phase transition in methane and its modifications.

4.13 THE OPTICAL ABSORPTION OF Mn^{2+} IN CUBIC AND TETRAGONAL CRYSTAL FIELDS

D.H. Goode, Department of Physics, University of British Columbia.

The fine line absorption spectra of the Mn^{2+} ion in $\text{MnCl}_2 \cdot 6\text{NH}_3$, $\text{MnCl}_2 \cdot 2\text{H}_2\text{O}$, $\text{KCl} \cdot \text{MnCl}_2 \cdot 2\text{H}_2\text{O}$ and $n\text{NH}_4\text{Cl} \cdot \text{MnCl}_2 \cdot 2\text{H}_2\text{O}$ have been measured at low temperatures. The ion lies at a site of cubic symmetry in the amine and approximate tetragonal symmetry in the hydrates. A cubic ligand field calculation has been made for the d^5 configuration which includes spin orbit coupling and with it the level splittings and doublet intensities are discussed. The calculations were further extended to include a tetragonal distortion and were then able to reproduce reasonably well the fine structure in the 4T_2 level of the hydrates observed at 27,000 cm^{-1} .

4.14 ATOMISTIC MECHANISM OF THE FERROELECTRIC BEHAVIOUR OF COLEMANITE

F.N. Hainsworth and H.E. Petch, Department of Physics, Hamilton College, McMaster University.

A neutron diffraction study of the hydrated borate mineral colemanite ($\text{CaB}_3\text{O}_4(\text{OH}) \cdot \text{H}_2\text{O}$) has been carried out at room temperature and at -20°C, primarily to determine the positions of the hydrogen atoms above and below the ferroelectric transition temperature of -2.50°C. Most of the hydrogen bonds in colemanite are of quite normal character and do not change appreciably through the transition. However, one of the hydrogen atoms of the water molecule and the hydrogen atom of an adjacent hydroxyl group, which are in a state of dynamic disorder at room temperature, are found to settle into ordered, non-centrosymmetric positions below the Curie point. Some of the other atoms are found to undergo small, but in some cases significant, displacements from their room temperature positions. Assuming a reasonable distribution of charges, the magnitude of the spontaneous

polarization calculated from the observed positional changes is comparable to the measured value. These results have been used to develop a qualitative theory of the mechanism of the transition from the atomistic point of view.

Thursday, June 10, 9:00 a.m.

Hennings 201

Session 5. EXPERIMENTAL NUCLEAR PHYSICS I

CHAIRMAN: R.E. Bell

5.1 FAST PHOTONEUTRON ANGULAR DISTRIBUTIONS

S.M. Hussain and K.B. McNeill, Department of Physics, University of Toronto.

Angular distributions of fast photoneutrons produced from nuclei irradiated with 22 MeV bremsstrahlung have been measured using the reaction $S_{-1}^{20}(np)Al^{20}$ as a threshold detector. The intensity of the 1.78 MeV gamma rays produced after the decay of the Al^{20} was used as a measure of fast neutron flux. Results will be presented for nuclei in the region $N = 20$ to $N = 65$.

5.2 NUCLEAR ISOMERISM IN THE MILLISECOND RANGE

Rezso L. Kovacs, Foster Radiation Laboratory, McGill University.

Five new isomers have been observed in a pulsed 100 MeV proton beam survey of eleven elements. Four of these isomers were examined in detail. The new isomers are:

Target	Half-life (ms)	γ -ray energy (keV)	Isomers
Bi	53	160, <u>580</u> , 720	Po ^{205m₂}
Sb	110	<u>280</u>	Te ^{117m}
Ho	53	<u>160</u>	Ho ^{156m}
Tb	15.5	90, <u>150</u>	Dy ^{157m}
Gd	25	<u>90</u>	not assigned

Assignments are made on the basis of energy thresholds of production and K x-ray absorption measurements. A decay scheme for Po^{205m₂} is presented.

5.3 BETA-GAMMA ANGULAR CORRELATION IN As⁷⁴

E. Habia, H. Ogata, W. Armstrong, Physics Department, Assumption University, Windsor.

The beta-gamma directional correlations for the first forbidden decays $As^{74}\beta^{-}Se^{74}$ and $As^{74}\beta^{-}Ge^{74}$ have been investigated.

For the sequence $(2^{-}) (\beta^{-}) (2^{+}) (\gamma) (0)$ the reduced A_2 coefficient is small. For the sequence $(2^{-}) (\beta^{-}) (\gamma) (2^{+}) (0)$ the A_2 coefficient is linear with p^2/w and the reduced coefficient is $-.022 \pm .001$.

Possible values of matrix elements have been calculated for this case.

5.4 LIFETIMES OF THE 1.74, 2.15, AND 3.59 MEV STATES IN B^{10}

R.E. Azuma and K.P. Jackson, University of Toronto.

Preliminary experiments have been conducted to measure the mean gamma ray lifetimes of the 1.74, 2.15 and 3.59 Mev states in B^{10} . The general method employed was that of attenuated Doppler shift measurement. In these experiments multichannel analyser routing and coincidence techniques were used to eliminate some of the uncertainties in such results due to possible energy instability in the gamma ray detection system. The initial results indicate:

1.74 Mev State: $\tau < 2 \times 10^{-13}$ Sec.

2.15 Mev State: $8 < \tau < 25 \times 10^{-13}$ Sec.

3.59 Mev State: $1.4 < \tau < 5 \times 10^{-13}$ Sec.

The observed transition probabilities are compared with detailed shell model predictions of Kurath.

5.5 INVESTIGATION OF THE LOW-LYING LEVELS OF Cl^{35}

P. Taras and R.E. Azuma, University of Toronto.

The spins, parities, mixing ratios and branching ratios of the following six levels in Cl^{35} were measured: 1.22 Mev, 3.00 Mev, 3.16 Mev, 4.17 Mev, 7.544 Mev and 7.844 Mev. These levels were populated by means of the $S^{34}(p, \gamma)Cl^{35}$ reaction at two resonances. The proton beam was obtained from the Princess Margaret Hospital 3 Mev Van de Graaff. The decay γ -ray cascades were examined utilizing the technique of triple angular correlation and sum coincidence methods. Two 5" x 4" NaI counters were used in these experiments.

5.6 SPINS OF THE 2.14 AND 5.03 MEV STATES IN B^{11} FROM ANGULAR CORRELATION MEASUREMENTS IN $B^{10}(dp)B^{11}$ *

B.A. Whalen and B.L. White, Department of Physics, University of British Columbia.

*The 5.03 Mev state in B^{11} was excited by the reaction $B^{10}(dp)B^{11}$, using 1.5 Mev deuterons from the U.B.C. Van de Graaff accelerator. This state decays by gamma emission direct to the ground state (γ_1) and also by a cascade through the 2.14 Mev first excited state (γ_2 and γ_3). Angular correlations ($p-\gamma_1$), ($p-\gamma_2$), and ($p-\gamma_2-\gamma_3$) were measured. The only spin assignments consistent with the correlation results are (1/2) for the 2.14 Mev state and (3/2) for the 5.03 state. These assignments are not dependent upon arguments concerning γ branching ratios. The population parameters of the 5.03 state have been determined from the correlation measurements and are compared with the predictions of (d,p) reaction theories.

5.7 THE DECAY SCHEME OF Sn¹¹³

J. Ungrin and K.I. Roulston, University of Manitoba.

The intensities of the gamma rays of In¹¹³ following the decay of Sn¹¹³ by electron capture have been measured relative to the 393 keV gamma ray (100) and found to be 2.4 for the 257 keV gamma ray and 0.1 for the 650 keV gamma ray. The end-point of the inner bremsstrahlung spectrum has also been determined.

5.8 ELECTRONIC MASS SORTING OF (p,p') AND (p,d) REACTIONS AT 100 MeV

S.K. Mark and R.B. Moore, Foster Radiation Laboratory, McGill University.

A high speed electronic system for the identification of charged particles (proton, deuteron, triton, etc.) resulting from nuclear reactions induced by 100 MeV protons has been developed based on a simultaneous determination of dE/dx and E using plastic scintillators. The system is capable of separating charged particles over an energy range between 20 MeV and 100 MeV, with a maximum dead time of 0.8 μ s. It has been used in an experiment to study scattered protons and pick-up deuterons from a number of nuclei. In each bombardment both proton and deuteron counts are accumulated concurrently. Angular distributions for the proton and deuteron groups of different energies, resulting from proton induced reactions in Carbon nuclei, are presented. Energy resolution of 1.5% for 100 MeV protons and 1.8% for 85 MeV deuterons were obtained.

5.9 EVIDENCE FOR THE EXISTENCE OF THE DIPROTON STATE IN THE He³(He³,2p)He⁴ REACTION

E.W. Blackmore and J.B. Warren, Department of Physics, University of British Columbia.

The mechanism of the He³(He³,2p)He⁴ reaction has been studied at $E_{He^3} = 1.15$ MeV by observing the angular distribution of coincidence events between the two final state protons and the coincidence proton spectra for various angles between protons. The data indicates that the dominate process is the sequential decay through the ground state of Li². Good evidence is found for the existence of a broad diproton state, unbound by approximately 600 keV.

5.10 NEUTRON PRODUCTION IN THICK TARGETS BOMBARDED BY HIGH ENERGY PROTONS

J.S. Fraser, R.E. Green, J.W. Hilborn, and J.C.D. Milton, Atomic Energy of Canada Ltd., W.A. Gibson, E.E. Gross, and A. Zucker, Oak Ridge National Laboratory.

Neutron production by protons (0.5 to 2.0 BeV) in thick targets of Be, Sn, Pb and depleted U has been measured in the external beam of the Brookhaven Cosmotron. The targets were located in a large tank of H₂O.

Beam current was measured by the $C^{12}(p,pn)C^{11}$ reaction; neutron production by foil activations in the H_2O and an integrating vanadium β -current detector.¹⁾

The table lists results from a preliminary analysis of the data for 10.2 cm diam x 61 cm long targets of Pb and U. Neutron fluxes are maximum values at radial positions of 0.8 cm and 12.8 cm from the surface of the target, normalized to a proton beam current of 65 ma, which has been proposed for the Intense Neutron Generator.²⁾ The use of D_2O as moderator in ING will mean an increase both in the maximum flux and the volume of high flux compared to H_2O moderator.

Proton Energy BeV	Yield 10.2cm Pb n/p	nv_U ($n/cm^2/sec$) $\times 10^{-16}$			
		10.2cm Pb		10.2cm U	
		r=6cm	r=18cm	r=6cm	r=18cm
0.54	9.0	0.71	0.130	1.10	0.259
0.72	13.3	0.94	0.176	1.70	0.409
0.96	17.6	1.19	0.223	2.18	0.543
1.00	19.6	-	-	-	-
1.47	29.4	1.77	0.331	2.97	0.718
1.98	42.5	-	-	-	-

1) J.W. Hilborn, *Nucleonics* 22, 69 (1964)

2) G.A. Bartholomew, J.C.D. Milton and E.W. Vogt, AECL-2059 (1964)

5.11 DIRECT CAPTURE MODEL FOR THE $D(p,\gamma)He^3$ REACTION WITH APPLICATION TO THE PHOTODISINTEGRATION OF He^3

G.M. Bailey, G.M. Griffiths, and Malcolm McMillan, Department of Physics, University of British Columbia.

A two body direct-capture model has been used to calculate cross sections for the reaction $D(p,\gamma)He^3$ for the energy range 25 keV-16 MeV. A simple square well was used for the nuclear potential and contributions to the radiative matrix elements from interior and exterior regions were included. A good fit to the p-wave capture cross section can be obtained at low energies by assuming a zero phase shift and an interaction radius of 4.35 fm. for the $D + p$ system. Extension of these calculations to higher energies gives a surprisingly good fit to the $E1$ total photodisintegration cross section for the inverse reaction $He^3(\gamma,p)D$; the agreement being within 10% from the threshold to 16 MeV.

A calculation was also made of the magnetic dipole S-wave capture cross section using the same model. The model is questionable in this case since it does not reproduce the observed magnetic moment of He^3 . The results reproduce the observed energy dependence satisfactorily, and the cross section is high by a factor of six.

Thursday, June 10, 1:45 p.m.

Hebb Theatre

Presidential Address and business meeting. (N.B. starts at 1:45).

Discours du président et réunion plénière (N.B. commence à 1:45 hre.)

Thursday, June 10, 4:30 p.m.

Hebb Theatre Steps

Tour to Simon Fraser University

Thursday, June 10, 8:30 p.m.

Hebb Theatre

Musical Evening. Vocal and instrumental selections by Mrs. Challice, Mrs. Krause, Mrs. Williams, Dr. Herzberg, and Dr. Welsh.

Friday, June 11, 9:00 a.m.

Hebb 10

Session 6. Symposium on CRUSTAL STRUCTURES IN CANADA

Chairman: E.R. Kanasewich

6.1 SEISMIC EXPLOSION STUDIES OF CRUSTAL STRUCTURE IN WESTERN BRITISH COLUMBIA

W.R.H. White, Dominion Astrophysical Observatory, Victoria.

Seismic explosion studies along the west coast of British Columbia have indicated a crustal section of about 50 km. thickness for a line along the east side of Vancouver Island. The result is based on the absence of Pn as a first arrival to a distance of 350 km. A number of short profiles have consistently revealed the presence of an intermediate layer with a compressional wave velocity of about 6.8 km/sec., at a depth of from 5 km. to 11 km. below the surface in the Vancouver Island area. Records obtained from the Ripple Rock explosion to the east and more recent studies in the interior plateau area indicate a thinning of the crust to about 30 km.

6.2 SEISMIC REFRACTION STUDIES IN ALBERTA

G.L. Cumming, Department of Physics, University of Alberta, Edmonton.

Seismic measurements of crustal thickness have been made along a line 750 km long from Swift Current, Saskatchewan to Arrowhead, British Columbia. These indicate a generally thick crust of nearly 50 km under southern Alberta with an indication of a thinner crust beginning at the eastern margin of the Rocky Mountains.

Data from explosions in Lake Superior, recorded in Alberta, indicate the presence of a low velocity layer in the mantle at a depth of approximately 120 km and a thickness of the order of 30 km and show the feasibility of making refraction measurements at very long range, from selected shot locations.

Power spectra of several series of shots have been obtained, which indicate very little change in frequency content over distances of 200 km. Shot environment appears to have a much greater effect than any variations due to distance.

6.3 THE GRAVITY FIELD OF ONTARIO IN THE LAKE SUPERIOR-JAMES BAY REGION

J.R. Weber, A.K. Goodacre, R.K. McConnell, Dominion Observatory, Ontario.

During the past two summers regional gravity mapping of Ontario was carried out with the observation of some 200 reconnaissance underwater gravity stations over Lake Superior and extensive measurements over the linear zone of positive gravity anomalies between Chapleau and Moosonee, Ontario, known as the Kapuskasing Gravity High. In general the gravity field over the Superior Basin correlate well with the known surface geology; positive anomalies correlate with middle Keweenawan lava flows while negative anomalies tend to correlate with late Keweenawan sediments and low density PreCambrian granites. The large positive Bouguer anomalies indicate the presence of high density rocks within the crustal column underlying Lake Superior.

Recent investigations strengthen the hypothesis that the Kapuskasing feature is the expression of crustal rifting of continental significance. The anomalies cut across and show no obvious relation to the structural trends of the surface rocks. Alkaline intrusions commonly associated with crustal rifting lie along the anomaly axis. Extension of rifting to the north and south and the significance of the feature in relation to Lake Superior and the Michigan basin are examined.

6.4 THE CONVERTED-WAVE METHOD OF REFRACTION INTERPRETATION FOR AN ARBITRARY VELOCITY VS. DEPTH LAW

D.H. Hall, Department of Geology, University of Manitoba.

In crustal seismic refraction surveys, where interpretation is based on traveltimes, converted waves make possible a very much greater yield of information than can be obtained from a single wavetype. It is possible, on combining longitudinal and converted head-wave traveltimes, to make some degree of distinction between the effects of varying layer thickness in a layered medium and those of varying velocity with depth. Such a distinction is not possible with a single wave type when head-waves are used alone.

The potentialities of the converted-wave method of re-

fraction interpretation in the case of an arbitrary velocity vs. depth law are investigated, and illustrated with examples from crustal seismic refraction surveys in Canada.

6.5 PHYSICAL EVOLUTION OF THE CANADIAN ARCHAEOAN GRANITIC CRUST

H.D.B. Wilson, University of Manitoba.

Regional geology, geophysics and geochemistry show the physical nature and evolution of the granitic portion of the crust in the Archaean core of the Canadian shield. A range of erosional levels from 8 to 30 km. above the base of the granitic layer are now recognizable. The lowest layer consists of partially melted sedimentary rocks overlain by a thick continental orogenic volcanic series. Volcanism was followed or accompanied by the rise of piercement domes of Kenoran age granite which originated by melting of the sedimentary series near the base of the granitic crust.

Following the single cycle of sedimentation, volcanisms and granite intrusion, the crust has remained relatively stable for the last 2.5 billion years. It has, however, been cut by the relatively narrow orogenic Kapuskasing gneissic belt and the Penokean fold belt. The stable crust has also failed by non-orogenic fracture under tensional stress during at least five different periods. Flood basalts originating at unknown depths rose through the tensional fractures. The stable crust has also been pierced by many non-orogenic alkaline volcanic necks whose age, origin, and structural relations are not yet known. The source of the major volcanic chemical types is a major geophysical problem.

The evolution, rock types, and structure of the Canadian, Western Australian, and Southern Rhodesian Archaean shields are identical, but are unlike those of later geological periods. The removal of vast amounts of material from the Archaean core by erosion is compatible with a growing continent.

6.6 INTERPRETATION TECHNIQUES AND THE LAKE SUPERIOR EXPERIMENT

M.J. Berry and G.F. West, University of Toronto.

The time-term method has often been suggested as a direct and objective approach to the interpretation of first arrival times when the redundancy of data is high. The Lake Superior Experiment of 1963 has provided an opportunity to test the method and has shown it to be eminently successful. An Upper Refractor has been mapped and the analysis reveals it to have a basin structure, with the surface outcropping at the edges of the Lake, and a depth of approximately 10 km. in the centre. On the assumption of uniform layer velocities the Mohorovicic discontinuity is revealed as a surface with considerable topographic relief, having depths under the west and east coasts of 30 and 50 km respectively.

Brekhovskikh's and Heelan's method for determining the

amplitudes of reflected and head waves has been reviewed and developed for layered media. Numerical calculations have been made for the case of two homogeneous layers above a half space. Using the velocity structure determined by the time-term study, the calculations suggest the distances ranges in which one might expect to detect the various normal and converted body waves. The records of the Lake Superior Experiment have been re-examined on this basis.

6.7 A MULTI-LAYER CONDUCTING EARTH IN THE FIELD OF PLANE WAVES

H.W. Dosso, Department of Physics, University of Victoria.

An n -layer plane conducting earth in the field of plane electromagnetic waves is treated. Each of several deep layers is divided into a sufficient number of sub-layers, with changing conductivity, to represent to a very good approximation a continuous change in conductivity. The amplitudes and phases of the electric and magnetic field components have been computed for several different conductivity distributions. Initial calculations have been made for structures with as many as 1000 horizontal conducting layers, and a frequency of 1 cycle/sec.

6.8 PALAEO-INERTIA OF THE EARTH'S CRUST

E.R. Deutsch, Department of Physics, Memorial University of Newfoundland.

Geological processes may alter significantly the moment of inertia of the crust. In Gold's model of a plastically yielding Earth a relatively modest redistribution of mass could provoke polar wandering at 10^3 - 10^4 cm/y. Such motions have never been clearly recorded by palaeomagnetism, which supports continental drift averaging a few cm/y. since the Precambrian. Before attempting an explanation, one might estimate the polar shift that should have resulted from specified crustal rearrangements. An estimate based on disruption of hypothetical supercontinents is presented here. The Milankovitch model was adopted, with standard, tabular continental sections in perfect isostatic equilibrium with standard oceanic crust, and smoothed coastlines parallel to latitude circles or meridians.

The results, obtained on the University's IBM 1620 computer, indicate that typical shifts of the figure poles are smaller than the crustal displacements invoked as their cause. It appears that polar wandering would be restrained (i) by the diversity of mass distribution prior to drift, and (ii) by partial compensation of torques contributed by the drifting crustal blocks. The effective mass asymmetry is perhaps in the mantle, so that the spin axis may be actually aligned with a resultant of the figure axes of mantle and crust.

Session 7. CANADIAN PHYSICS (and contributed papers in general physics)

Chairman: F.T. Davies

7.1 THE CANADIAN RESEARCH ENVIRONMENT (45 min.)

J.R. Whitehead, Deputy Director, Scientific Secretariat, Ottawa.

7.2 INTENSE NEUTRON GENERATOR BASED ON A PROTON ACCELERATOR (45 min.)

G.A. Bartholomew, Chalk River Nuclear Laboratories.

7.3 SPECTRA OF POSITRON LIFETIMES IN THE ALKALI HALIDES

R. Barton and E.J. Neuheimer, Loyola College, Montreal, and Foster Radiation Laboratory, McGill University.

The spectrum of positron lifetime against annihilation has been measured, by the delayed coincidence method, for positrons annihilating in 12 of the alkali halides. A ^{22}Na source of positrons, deposited on a thin (about $200\ \mu\text{g}/\text{cm}^2$) gold foil, was sandwiched between layers of carefully dried sample material. In all cases the delayed coincidence spectrum exhibits at least 3 components. The curves may be still more complex, but, initially at least, they have been fit with the sum of 3 exponentials. All results are similar. For example, preliminary results for NaCl are

$$\tau_1 = 2.1 \times 10^{-10} \text{ s} \quad I_1 = 45\%$$

$$\tau_2 = 4.4 \times 10^{-10} \text{ s} \quad I_2 = 54\%$$

$$\tau_3 = 11 \times 10^{-10} \text{ s} \quad I_3 = 1\%$$

7.4 TOTAL REFLECTION OF 3-cm MICROWAVES

H.C. Bezner and A.B. McLay, McMaster University.

The radiation field of a rectangular horn fed by 3-cm microwaves from a klystron oscillator has been investigated with a small crystal diode detector (a) after total reflection from the hypotenuse face of a 45° - 90° - 45° dielectric prism; (b) behind the hypotenuse face. Sideways displacement of the totally reflected beam of the order of the wave-length has been observed for each of several angles of incidence greater than the critical angle $36^\circ 30'$ in the dielectric. The results are in agreement with similar displacements first observed by Goos and Hänchen¹⁾, using visible monochromatic light, internally reflected about 65 times in a parallel-sided glass plate to obtain a measurable effect.

The measurements are in qualitative agreement with a

theory proposed by Artmann²⁾, applicable very close to the critical angle, except that there is some distortion of the field pattern probably resulting from small divergence of the microwave beam. Agreement with theory is much better for angles of incidence greater than 40° , using a more generally applicable equation derived by Renard³⁾.

The totally reflected patterns are compared with respective patterns observed behind the totally reflecting surface, which show an expected evanescent wave fall-off of intensity with distance away.

- 1) Ann.Physik 1, 333(1947); 5, 251(1949).
- 2) Ann.Physik 2, 87(1948).
- 3) J. Opt. Soc. Amer. 54, 1190(1964).

7.5 DECOMPRESSION PROBLEMS AND ANALOGUE SIMULATION IN OPERATIONAL DIVING

R.S. Weaver, Defence Research Medical Laboratories, Wing Commander R.A. Stubbs and Surgeon Lieutenant Commander D.J. Kidd, Institute of Aviation Medicine.

The problem of safe and efficient decompression following single or repetitive dives to various depths has been studied intensively in the past, but using biochemical principles has invariably led to insoluble or incorrect results. The present work, in which the formation of gas bubbles in the tissues is considered on the basis of straight-forward physical principles, has led to the development of a pneumatic computer which functions as an analogue of the body tissues. The effectiveness of this computer has been proven in several hundred tests in a hyperbaric chamber. To permit simulation of such dives in the laboratory on an accelerated time scale, an electrical analogue diving computer has been constructed, in which resistors and capacitors are the equivalents of diffusion resistance and tissue gas solubility in the body. Theoretical analyses of the electrical analogue for any number of circuit elements have been compared with actual results from dives, and the electrical and analogous physiological parameters determined. To prevent bubble formation or "bends" on ascent from a dive, the external pressure (and by analogy the source voltage of the electrical system) must be a definite function of time. The theoretical continuous ascent function following a given dive profile has been derived in terms of exponential and Bessel functions. A voltage comparator circuit, which ensures that the applied source voltage never exceeds the voltage on any capacitor by more than the allowable ratio of gaseous supersaturation of body tissues has been incorporated in the electrical analogue to generate the ascent function.

7.6 ELECTRIC ANALOGUES OF MUSCLE FIBRES

C.E. Challice and T.A. Clark, University of Alberta, Calgary.

Circuits which simulate the electrical conduction characteristics of the neuron have been modified by the addition of feedback to simulate the electrical properties of the various forms of striated muscle, particularly some of the "specialized" tissues of the mammalian heart. The purpose of the analogues is to assist in relating the electrical properties with the structures observed by electron microscopy. It is suggested that there is electrical feedback in the muscle cells which is responsible for their electrical properties, and possible relationships between the feedback and observed structures are discussed. It is thought possible that further development of analogues might aid in supplying information on abnormalities and possibly aid in the remedying of them.

7.7 THE EFFECT OF DEUTERATION ON THE NEEL TEMPERATURE IN $\text{CoCl}_2 \cdot 6\text{H}_2\text{O}$

D.S. Sahri, Department of Physics, University of British Columbia.

The high accuracy which the use of nuclear magnetic resonance¹⁾ provides in determining the Neel temperature has been used to observe the changes in this transition point caused by deuteration in $\text{CoCl}_2 \cdot 6\text{H}_2\text{O}$. The Neel temperature is a periodic function of orientation of the magnetic field with respect to the crystal axes. Results will be presented showing that no change in the periodicity occurs upon increasing the percentage of deuteration. However, the following effects are observed.

- i) The Neel temperature in every orientation increases monotonically.
- ii) The range of the variation of the Neel temperature decreases.

The experiment was done by monitoring deuteron and proton resonance at a magnetic field of 5 kilogauss. These results are in qualitative agreement with the theory of Vlaslov²⁾, as discussed by Belov³⁾.

The nuclear magnetic resonance of protons and deuterons in deuterated crystals of $\text{CoCl}_2 \cdot 6\text{H}_2\text{O}$ will be discussed.

- 1) E. Sawatzky and M. Bloom, Can. J. Phys. 42, 675 (1963).
- 2) K.B. Vlaslov, Izv. Akad. Nauk, SSSR (Ser. Fiz.) 18, 339 (1954).
- 3) K.P. Belov, Magnetic Transitions, pp.127-30 Consultant Bureau, New York.

Session 8. UPPER ATMOSPHERIC PHYSICS

Chairman: B.W. Currie

8.1 OBSERVATIONS OF THE OXYGEN RED LINE IN THE DAYGLOW

L.L. Cogger and G.G. Shepherd, University of Saskatchewan.

Observations on the dayglow emission at 6300 Å have been carried out at Saskatoon since 1962, using a spectrometer consisting of two Fabry-Perot etalons and a narrow passband interference filter. But unambiguous identification of OI 6300 Å has been possible only recently because of the presence of fraunhofer structure in the solar continuum. Also, the intensity of the emission relative to the background scattered light is much lower than predicted theoretically. Ground observations of this emission have also been reported by Noxon and by Jarrett and Hoey. Our results will be described and compared with theirs. A similar spectrometer, but with simultaneous recording on ten channels, is under construction and will be briefly described.

8.2 OBSERVATIONS ON THE RELEASE OF NITRIC OXIDE IN THE E-REGION

(Anonymous)

Nitric oxide gas has been released in the E-Region at two latitudes, two seasons and two times of day. Examination of radiation originating in reaction of the gas with ambient atomic oxygen indicates:

- 1) At E-Region pressures, the radiative reaction between NO and O may be a 2-body process, not a 3-body as current kinetic models suggest.
- 2) The measured intensity of the chemiluminescent radiation is greater than theory predicts, using rate constants based upon laboratory measurements. Inference is that the atmospheric and laboratory reaction processes are not the same.
- 3) The spectral content of the atmospheric radiation is not the same as laboratory radiation originating at a pressure of one millimeter, strengthening the suggestion that differences exist in the two processes.
- 4) The failure to obtain any chemiluminescent radiation below 78 km implies that atomic oxygen concentration drops sharply below 85 km, reaching a value at 78 km less than 1/50 maximum value.
- 5) The altitude at which emission intensity peaks is just short of 100 km, in agreement with photochemical theory.
- 6) The altitude of peak emission intensity appears to be higher at lower latitude.

- 7) No evidence was obtained of a diurnal or seasonal (spring-fall) effect on the altitude of peak emission intensity.

8.3 ATMOSPHERIC TIDE MEASUREMENTS BY COSMIC RAY INTENSITY

G.R. Mason and R.M. Pearce, Department of Physics, University of Victoria.

The air mass participating in atmospheric tides is commonly measured by pressure readings, but can also be observed in the changing attenuation of cosmic rays. The cosmic ray intensity measured in the first 250 days of operation of the Victoria neutron monitor has been Fourier analysed to obtain a preliminary value of the amplitude of the semidiurnal tide S2.

8.4 THE ANISOTROPY OF IONOSPHERIC IRREGULARITIES DEDUCED FROM VHF SCATTER MEASUREMENTS

G.F. Lyon, University of Western Ontario, London.

One of the least explored effects in auroral VHF scattering is the effect of the angle of incidence upon the received amplitude. The signals received on two VHF (40 Mc/s) scatter circuits of quite different geometries but viewing a common scattering region are compared. On the basis of theoretically predicted amplitude ratios for scattering from an assembly of gaussoidal scatterers it is confirmed that signals of the type previously characterized as A3 arise from nearly isotropic scatterers while signals of the type A1 or A2 arise from scatterers whose axial ratio is at least 10. The suggestion is made that scatterers may exist simultaneously at more than one level and that the character of the signal observed will depend markedly upon the geometry of the circuit used.

8.5 A NEW METHOD OF DETERMINING CROSS-CORRELATION COEFFICIENTS OF TIME-VARYING SIGNALS

F.H. Palmer and G.F. Lyon, University of Western Ontario, London.

Pulse counting techniques allow the cross-correlation coefficient between two time-varying signals to be rapidly evaluated if the two signals are first converted to pulse trains whose repetition frequencies are proportional to the respective amplitudes. Equipment using this technique is described. Provided the depth of modulation of the signals is over 50% the correlation coefficient may be determined to an accuracy of ± 0.05 for signal durations of only 2 minutes.

Some examples are shown of determinations of coefficients for VHF scatter signals received on spaced antennae. Such measurements may be related to the scale size of the ionospheric inhomogeneities responsible for the scattering.

8.6 MULTICHANNEL AURORAL PHOTOMETRY IN THE ARCTIC DURING THE I.Q.S.Y.

M.D. Watson, Radio and Electrical Engineering Division, National Research Council, Ottawa.

Auroral photometers have been operated at Resolute Bay and Baker Lake, N.W.T. and Great Whale River, Que., from September 1964 to May 1965. The photometers measured auroral intensities at 5577A, 4861A, and 3914A, over a field of view 15° square, with a time resolution of one minute. The results of a preliminary analysis of the records will be presented and discussed.

8.7 FREQUENCY VARIATION IN IONOSPHERIC CYCLOTRON HARMONIC SERIES OBTAINED BY THE ALOUETTE I SATELLITE

R.E. Barrington and Luise Herzberg, Defence Research Telecommunications Establishment, Radio Physics Laboratory, Ottawa.

Ionograms produced by the Alouette I topside sounder frequently show well developed series of cyclotron harmonics. Their frequencies have been determined from A (amplitude) scans with an accuracy of ~ 0.02 mcs for the sweep range of 1 to 6 mcs. In all cases examined the frequencies of all members of the harmonic series are within the experimental accuracy, integral multiples of the cyclotron frequency obtained from present knowledge of the earth's magnetic field strength at the satellite height. This is in contrast to the results of laboratory experiments by Crawford, Kino and Weiss which have yielded converging series of harmonics.

Resonance frequencies obtained theoretically by solving Bernstein's dispersion relation for electrostatic wave propagation, are in agreement with the laboratory data, if it is assumed that resonance occurs at frequencies for which the group velocity of the waves is zero. The known features of the Alouette cyclotron resonances are in agreement with the assumption that it is the antenna length which is important in determining their decay time and frequency dependence. The satellite and laboratory experiments may possibly be reconciled by considering the large difference in the ratio of antenna length to electron gyro radius of the two experiments.

8.8 AN IONOSPHERIC ELECTRON CYCLOTRON RESONANCE PHENOMENON OBSERVED BY ALOUETTE

E.L. Hagg and D.B. Muldrew, Defence Research Telecommunications Establishment, Defence Research Board, Ottawa.

An unexpected reflection trace is often observed on high latitude spread F ionograms recorded by the Alouette sweep-frequency topside sounder. From this trace it has been deduced that the radio energy transmitted on a particular frequency causes electron cyclotron resonance at one half the frequency of the transmitted wave at a height of a few hundred kilometers or less below the satellite. The trace is explained

by a model in which this resonance subsequently generates a second harmonic wave equal in frequency to the original transmitted wave.

8.9 STUDIES IN LOW FREQUENCY PROPAGATION AT 80 Kc/s

D.B. Ross, G.L. Goodwin, J.S. Belrose, Defence Research Telecommunications Establishment, Defence Research Board, Ottawa.

A present problem in low frequency radio wave propagation is the prediction of the field strength and phase variations with distance of the received radio wave. In theory the total field may be regarded as being either as a combination of several modes propagated in the earth - ionosphere waveguide, or as the vector sum of a ground ray plus several rays reflected between earth and ionosphere.

Transmissions received at fixed distances characteristically show oscillations in field strength when the ionospheric reflection height is changing. An interpretation of these oscillations requires a knowledge of which propagation modes predominate at these distances.

Observations in an aircraft of the variation with distance to 1800 km of the signal from an 80 Kc/s transmitter at Ottawa were obtained in October, 1964. These observations are related to several ground-based observations, and are compared to theoretical predictions of low frequency propagation by Volland (1964).*

* H. Volland, "Bemerkungen zur Austinschen Formel", NTZ 12, 641 (1964).

8.10 A CORRELATION BETWEEN THE OCCURRENCE OF ABRUPT INCREASES IN THE INTENSITY OF BREMSSTRAHLUNG X-RAYS AT BALLOON ALTITUDES AND TYPE B AURORAL FORMS DURING INTENSE POLAR SUBSTORMS

T.A. Clark and C.D. Anger, Department of Physics, University of Alberta, Calgary.

A balloon-borne x-ray detector was at operating altitude over Fort Churchill during the break-up phase of several polar geomagnetic substorms. During this time several abrupt and intense increases in x-ray intensity were observed to occur in close time correlation with visual reports of auroral forms exhibiting intense red lower borders characteristic of type B aurora.

8.11 OBSERVATIONS OF THE PROFILE OF THE NORTHERN BORDER OF ELECTRON PRECIPITATION DURING SEVERAL POLAR MAGNETIC SUBSTORMS

T.A. Clark and C.D. Anger, Department of Physics, University of Alberta, Calgary.

Balloon measurements of the intensity of auroral x-rays produced by electron precipitation during several break-up phases of a polar substorm have been analyzed. A comparison

of x-ray intensity and energy spectrum information with magnetometer and riometer data and with visual observations indicates that at the onset of each break-up the balloon was north of the sharp precipitation boundary inferred from satellite data. It is suggested that subsequent magnetic activity swept this border over the balloon and thus provided a profile of electron precipitation through the border. Conclusions drawn from these data are compared with similar conclusions drawn from satellite measurements.

8.12 INVESTIGATIONS OF X-RAY INCREASES AT BALLOON ALTITUDES AND THEIR ASSOCIATION WITH RAPIDLY CHANGING AURORAL FORMS AS PHOTOGRAPHED BY A MECHANICAL FLYING SPOT SCANNER

G.R. Pilkington, C.D. Anger, and T.A. Clark, Department of Physics, University of Alberta, Calgary.

High speed photographs of an auroral break-up (approximately Brightness II) at Churchill, Manitoba on the night of April 21 - 22, 1964 were compared with simultaneous data obtained from a balloon-borne x-ray detector. The pictures were taken using a mechanical flying spot scanner, which mechanically scanned over an area of the sky subtending an angle of 120° by 120° , with an angular resolution of 2° . The light from each picture element passed through a narrow band 5577A interference filter and fell onto a photomultiplier. A picture was simultaneously reproduced on an oscilloscope screen and photographed. Pictures were taken at the rate of approximately one per second during the break-up, which lasted about 18 minutes.

Out of thirteen detectable increases or decreases in x-ray intensity, corresponding changes in auroral luminosity were observed on nine occasions. On two other occasions, there is evidence that auroral intensity changes occurred outside the scanner field of view. Two events cannot be convincingly accounted for.

8.13 THE ${}^1\Delta_g - {}^3\Sigma_g^-$ O₂ BANDS IN THE TWILIGHT AND DAY AIRGLOW

R.L. Gattinger and A. Vallance Jones, Institute of Upper Atmospheric Physics, Department of Physics, University of Saskatchewan, Saskatoon.

A four-fold decrease has been observed in the maximum brightness of the $0-1 {}^1\Delta_g - {}^3\Sigma_g^-$ from 1960 to 1964. There is some indication that the brightness may depend on the monthly average sunspot number. Airborne observations of the $0-0$ band reported by Noxon and Vallance Jones, are presented in detail. The 1963 solar eclipse observations of Noxon and Markham are also presented in full. The calculations previously reported by Vallance Jones and Gattinger of the predicted brightness of the emission on the basis of the Hartley dissociation of ozone have been extended to cover the case of the solar eclipse. The predictions are not inconsistent with

the dayglow eclipse observation. The results to date suggest that the dayglow may not show the strong seasonal minimum in the summer observed for the twilight emission. Further observations made during the morning twilight confirm that the emission is much weaker than predicted in the morning. No explanation has been found of the seasonal, annual or evening-morning variation despite the consideration of several alternative excitation hypothesis.

The research reported in this paper was supported by the Air Force Cambridge Research Center, Office of Aerospace Research, U.S. Air Force, under Contract AF19(628)-2829.

Friday, June 11. 9:00 a.m.

Hennings 201

Session 9. APPARATUS OF NUCLEAR PHYSICS

Chairman: L. Katy

9.1 ATOMIC BEAM METHOD FOR PRODUCING A POLARIZED He^3 BEAM*

D. Axen, J.B. Warren, K.L. Erdman, and M.K. Craddock, Department of Physics, University of British Columbia.

An atomic beam apparatus designed to produce a polarized He^{3+} beam with an intensity of approximately one micro ampere is described. A Laval nozzle, cooled to 2.2°K, is used to produce a supersonic beam of He^0 atoms of Mach number 4. A hexapole magnet is used to focus the atoms in one of the two nuclear spin substates and defocus the other. The polarized atoms are then ionized by electron bombardment. The nuclear polarization of the resulting He^{3+} ions depends on the external magnetic field strength, being 50% in a weak field and 90% in a field of 6000 gauss. This field must be applied both at the ionizer and at the target region. Experimental results of the performance of the apparatus will be presented.

* Research supported by a grant from Atomic Energy of Canada Ltd.

9.2 SOME RECENT ADVANCES IN NUCLEAR ELECTRONICS

W.B. Reid and R.H. Hummel, Nuclear Enterprises Ltd., Winnipeg, K.I. Roulston, University of Manitoba.

The use of a time-to-amplitude converter in conjunction with a single channel analyzer for the fast coincidence circuit in a fast-slow coincidence system has been demonstrated¹⁾. Some useful modifications to the circuit described in reference¹⁾ which, allow the circuit (a) to be used in either the start-stop or pulse overlap mode and (b) allow conversion times as long as several microseconds to be used have been made. The design of a coincidence system using this TAC in conjunction with double delay line amplifiers and cross-over-pick-off circuits is described. Measurements of resolving time of the system as a function of photomultiplier noise and particle energy are presented.

A new ratio computer²⁾ has been further developed. This instrument calculates the amplitude ratio of two coincident pulses in less than 2 microseconds. Basic features of this circuit and some of its applications will be discussed.

- 1) R.B. Tomlinson and R.L. Brown, IEEE Transactions on Nuclear Science NS-11, 2, 28 (1964).
- 2) E.A. Gere and G.L. Miller, IEEE Transactions on Nuclear Science NS-11, 3, 382 (1964).

9.3 A COMPARISON OF NE 102 AND NE 103 PLASTIC PHOSPHORS

W.B. Reid and P. Leggate, Nuclear Enterprises Ltd., Winnipeg.

NE 103 differs from the familiar NE 102 plastic phosphor in that its fluorescence is predominantly green with a peak at 5050 angstroms as compared to 4250 angstroms for the peak emission of NE 102. The pulse shape, fluorescence spectra, relative response of various photomultiplier tube types, behavior of light collection efficiency as a function of scintillator size, light transmission of long rods and light transmission through commonly used light pipe material have been studied. It is found that NE 103 offers a significant advantage over NE 102 when it is required to use long light pipes between the phosphor and photo cathode.

9.4 PULSE SHAPE DISCRIMINATION IN ORGANIC SCINTILLATORS

W.B. Reid and R.H. Hummel, Nuclear Enterprises Ltd., Winnipeg.

A simple circuit for studying organic scintillators which derives a "fast" signal proportional to the peak amplitude of the anode pulse of a 56AVP and a "linear" signal proportional to the total charge collected, or pulse height of the same event is described. Relative pulse shapes can be determined by comparing the amplitude of the fast signal obtained from protons or alpha particles to the amplitude of the fast pulse produced by electrons which give rise to the same linear pulse height. Results of a comparison of NE 213 to NE 102, and NE 103 plastic scintillators and NE 223 and NE 224 liquid scintillators and stilbene will be presented.

The possibility of using this simple circuit in conjunction with computer analysis to determine the origin of the event is discussed.

9.5 THE PREPARATION OF LARGE LI-DRIFTED-GE DETECTORS

J. Fiedler, W.V. Prestwich, and T.J. Kennett, McMaster University.

The important advantages of Li-drifted Ge detectors are well known. The desirability of large-volume counters is also obvious. In order to achieve large-volume counters in the simplest way possible a new method has been successfully developed. The procedure allows one to alloy and to drift the

lithium into a large germanium crystal from all but one side.

In this new technique the lithium is deposited on the germanium crystal electrolytically from a molten mixture of Li Cl/K Cl. Since the salt bath has a melting temperature just above 400°C, the lithium is deposited and alloyed concurrently. The depth of the lithium alloy is easily controlled and all sides are alloyed simultaneously. Following this, the lithium is drifted from all but one side towards the centre of the germanium.

Various sizes of this "wrap around" counter were produced. The nature and distribution of the depleted region was determined by slicing and staining the detector. Typical results will be shown.

9.6 A He³ FILLED IONIZATION CHAMBER USED AS A NEUTRON DETECTOR

J.B. Warren and D.C. Healey, Department of Physics, University of British Columbia.

A He³ filled ionization chamber has been used at the University of British Columbia to measure the threshold energy of 1.13 MeV for Br⁸¹(p,n)Kr⁸¹ and to search for the source of the neutron background encountered in these measurements, a measurement of the cosmic neutron density at the earth's surface was made. This was found to be 4.2×10^{-9} n/cm³ over land and about 10% lower over the sea.

9.7 ACCURATELY COLLIMATED PARTIALLY POLARIZED 5 MEV NEUTRON BEAM

L.F.C. Monier, G.E. Tripard, and B.L. White, Department of Physics, University of British Columbia.

The apparatus described uses the D(d,n)He³ reaction at a bombarding energy of 2 Mev to produced a partially polarized (17%) 5 Mev neutron beam. The narrow-angle accurately collimated beam is obtained by using the associated particle method, developed from that previously used at a deuteron bombarding energy of 50 Kev¹⁾. This paper describes the improved apparatus required to detect the 300 Kev He³ recoil ions in an intense flux of coulomb scattered deuterons having energies up to 2 Mev. The results obtained with the apparatus are described.

1) B.L. White and L.F.C. Monier, Bull. Am. Phys. Soc, Series II, 8, 119 (1963).

9.8 A SEMICONDUCTOR DETECTOR FOR MEASURING STOPPING POWER AND RANGE-ENERGY RELATION FOR α -PARTICLES

E. Rotondi and K.W. Geiger, National Research Council of Canada, Ottawa.

A method has been developed to rapidly measure stopping power and range energy relation of α -particles in gases. The apparatus consists of a gas absorption cell in which α -particles

lose their energy and a semiconductor detector which determines the residual energy of the α -particles. Energies as low as 50 keV could be measured and the resolution of about 20 keV allows direct measurement of the energy distribution of originally monoenergetic α -particles as they traverse the gas. Since an ionisation chamber is not involved, the measurement of stopping powers is not affected by a variation of W (energy expended to produce an ion pair) with energy. For air, good agreement is shown with the range-energy relation of Jesse and Sadauskis who have assumed such a variation of W . Stopping powers for various hydrocarbons have also been determined to test Bragg's additivity law.

9.9 THE USE OF A TWO-PARAMETER PULSE-HEIGHT ANALYZER WITH A SUM-COINCIDENCE SCINTILLATION SPECTROMETER

J. Ungrin and K.I. Roulston, University of Manitoba.

The form of the spectral distribution to be expected from a sum-coincidence spectrometer, when the sum energy is displayed on one axis and the output from one detector is displayed on the other axis, is discussed. Rapid data acquisition permits investigation of weak and short-lived sources. Laborious searching for desirable sum-window levels is eliminated and corrections for drifts in angular correlation experiments can be applied, after the experimental data have been recorded.

The decay of Ba^{131} has been studied with the spectrometer.

9.10 DISTORTION OF TIME-DISTRIBUTIONS IN A DELAYED-COINCIDENCE TIME-ANALYZER

W.R. Wall and K.I. Roulston, University of Manitoba.

An analysis of the expected distortion of the time distribution of particles produced in bursts, when measured by a delayed-coincidence analyzer which is capable of analyzing not more than one particle per burst, is given. The distortion factor is the inverse transform of the correction factor which is applied to an experimental curve.

The problem of distortion is discussed with particular reference to the measurement of scintillation pulse shapes, although it has general application to neutron time-of-flight and short life-time measurements.

9.11 A METHOD OF APPLYING COMPTON SCATTERED NEUTRON CAPTURE RADIATION TO NUCLEAR PHOTO-EXCITATION

J.W. Knowles, Chalk River Nuclear Laboratories.

The source of ν -radiation consists of plates of titanium and nickel placed in an NRU beam tube. Characteristic (n, ν) radiations, in particular the 1.37 and 6.75 Mev ν -rays of Ti^{49} and the 8.99 Mev ν -rays of Ni^{59} are Compton scattered from a curved aluminum plate placed outside the reactor. The geometry

is arranged so that scattered radiation of one energy converges to a narrow beam at the position of the target. The energy of the convergent radiation is varied by moving the target to different angular positions with respect to the aluminum scatterer. The energy range is 0.1 to 8.5 Mev and energy selection 1-3%. The incident beam intensity is 1-10 quanta $eV^{-1} cm^{-2} sec^{-1}$. By varying the ν -ray beam energy between 6 and 8 Mev with approximately 2% energy selection, the elastic scattering and self-absorption of radiation from a target of natural lead has been measured. The elastically scattered radiation, detected by a NaI (Tl) scintillator at a mean scattering angle of 135° , shows intensity maxima corresponding to ν -ray transitions in lead at 6.6, 6.9 and 7.2 Mev. The elastic scattering results averaged over the 3 transitions gives an integrated cross-section over the energy width of the incident ν -ray beam of $(4 \pm 2) \times 10^3$ barns eV which can be interpreted to yield a total width for nuclear resonance scattering of 70 ± 30 eV. The self-absorption results give an average effective nuclear absorption cross-section for the 3 transitions in natural lead of 18 ± 5 barns.

9.12 SCINTILLATION DECAY IN CALCIUM TUNGSTATE

M. Sayer and W.R. Hardy, Queen's University, Kingston.

Values obtained by various authors for the luminescence decay time of calcium tungstate single crystals differ both in the magnitude of the decay time for a given type of excitation and in the possibility of pulse shape discrimination, i.e. the variation in decay time with type of incident particle. Measurements are reported for a range of pure and impurity-activated crystals excited by slow electrons, γ and α radiation. For all pure crystals a single exponential could be fitted to the decay. Significant changes in decay time with the type of incident radiation are noted for only a few of the crystals, representative values being 6.9 ± 0.3 , 6.0 ± 0.3 , and 4.1 ± 0.2 μsec for 7keV electrons, 1.33 MeV γ 's and 5.3 MeV α 's respectively. In general, it is found that crystals in which little discrimination between γ 's and α 's is observed show relatively large values of slow electron decay time, e.g. 6.8 ± 0.3 μsec for both types of particle versus 9.4 ± 0.3 μsec for electron excitation. This correlation and possible mechanisms for particle discrimination in calcium tungstate will be discussed in the light of additional experiments on the temperature dependence and thermoluminescence.

Friday, June 11, 2:00 p.m.

Hennings 202

Session 10. ASTRONOMY

Chairman: K.O. Wright

10.1 QUASARS (30 min.)

J.W. Moffat, University of Toronto.

10.2 THE 150-FOOT PRECISION RADIO TELESCOPE OF THE ALGONQUIN RADIO OBSERVATORY (20 min.)

W.A. Cumming, National Research Council, Ottawa.

10.3 SOLAR RADIO NOISE IN THE FREQUENCY RANGE 1.5 to 10 MC/S

T.R. Hartz, Radio Physics Laboratory, Defence Research Board, Ottawa.

Solar radio noise appears sporadically in the Alouette sweep-frequency recordings above the galactic noise level. The Type III bursts are the easiest to identify of the accepted noise classifications, and from a preliminary study of such bursts estimates have been made of the velocity of travel through the sun's corona of the exciting agency, and also of the temperature at various levels in the corona. Other types of solar noise can also be found in the recordings, and their characteristics in this frequency range are discussed briefly.

10.4 A NEW EQUIPMENT FOR INVESTIGATING THE POLARIZED COMPONENT OF GALACTIC RADIATION AT A FREQUENCY OF 850 Mc/s

V.A. Hughes, Department of Physics, Queen's University.

Most of the background radio-wave radiation is assumed to be due to synchrotron radiation from relativistic electrons accelerated in the weak magnetic field of the Galaxy, and should show a fairly high percentage polarization. Unfortunately, Faraday rotation and depolarization due to inhomogeneous magnetic fields reduce the value to a few percent. Nevertheless, a study of the magnitude and position angle of the polarized component at different frequencies should give some indication of the distribution of magnetic fields in the Galaxy.

Measurements by the Dutch group at 400 Mc/s and 610 Mc/s, obtained by the use of rotating dipoles at the focus of an 85 ft. diameter paraboloid, show two well defined regions of polarization, but spurious responses, due partly to lack of symmetry in the paraboloid and reflection from the ground, make most of the measurements unreliable. A completely new type of polarimeter has been built which overcomes a number of these difficulties. It consists of a static antenna array 100 ft. long which produces a reception pattern of $5^{\circ} \times 0.6^{\circ}$, by electronic means the received plane of polarization is made to rotate at a frequency of 1 Mc/s. The method and equipment will be described and it is hoped to show some of the results.

10.5 A RANDOM ARRAY FOR RADIO ASTRONOMICAL INVESTIGATION

V.A. Hughes, Department of Physics, Queen's University.

Large steerable parabolic antennas are expensive to build and various methods of synthesizing antennas are used. A new type of array, which produces a pencil beam, has been built and is being tested. It consists of 100 passive elements placed at random positions over the ground which scatter the received

radiation to a collecting antenna at the top of a 180-ft. tower. By adjusting the height of the individual elements, it is possible to steer the beam to different directions in the sky. The reception pattern is equivalent to that obtained with a paraboloid of diameter 300 ft. but the side-lobe peaks are considerably reduced. The array is being used for a detailed investigation of Galactic radiation at a frequency of 74 Mc/s.

10.6 **PRELIMINARY RESULTS ON THE NEUTRON ALBEDO INTENSITY ABOVE FORT CHURCHILL, CANADA**

G.A. Baird and B.G. Wilson, Department of Physics, University of Alberta, Calgary.

Rocket measurements of the neutron albedo radiation above Fort Churchill, Manitoba, have been made on two flights during 1964. The detector consisted of two scintillators, anthracene and plastic, with pulse discrimination selection between neutrons, gamma rays and charged particles. Neutrons are detected in the energy range 1 - 11 Mev. A differential energy spectrum of the form $dN/dE = kE^{-1.45} \pm 0.10$ was obtained over the range 2.7 - 11 Mev, in good agreement with the theoretical prediction. Two further flights have been made in March 1965 and the results will be presented at this meeting.

10.7 **ELECTRON FLUXES AT 1000 Km ASSOCIATED WITH THE 'TAIL' OF THE MAGNETOSPHERE**

I.B. McDiarmid and J.R. Burrows, National Research Council, Ottawa.

The outer Van Allen radiation zone at an altitude of 1000 Km usually exhibits a fairly well defined high latitude boundary as determined by a marked decrease in the intensity of 40 KeV electrons. At latitudes higher than the normal outer zone boundary the electron counters on board the Alouette satellite usually detect only a background rate corresponding to the galactic cosmic ray flux. However, on some occasions appreciable fluxes of electrons are observed at latitudes above what appears to be the boundary of the outer zone. The latitude profiles of these events are usually in the form of a narrow spike with some of the events having very high intensities; directional intensities of electrons above 40 KeV approaching $10^9 \text{cm}^{-2} \text{sec}^{-1} \text{sterad}^{-1}$ have been observed. The high latitude electron fluxes are found preferentially on the night side of the earth on lines of force which presumably connect to the 'tail' of the magnetosphere and at times when enhanced electron fluxes are observed in the trapping region of the outer radiation zone. It is suggested that electrons generated in the 'tail' of the magnetosphere may form an important source of electrons for the outer radiation zone.

10.8 THE CHANGE IN DIRECTION OF THE ANISOTROPY OF THE COSMIC RAY INTENSITY DURING THE PAST SOLAR ACTIVITY CYCLE

J. Katzman, National Research Council, Ottawa.

A small anisotropy exists in the cosmic ray intensity of about 0.3%. This anisotropy has been attributed by a number of authors to the magnetic fields of the sun that are drawn out by the solar wind and have shown theoretically that at no time can the direction of anisotropy lie in a direction making an angle of more than 90° with the sun-earth line. To determine the validity of this hypothesis it is best to study the diurnal hour of maximum of the cosmic ray intensity at a station near the geomagnetic pole. At a station such as Resolute Bay, (geomagnetic latitude 85°N) the area of sky through which primary particles pass forms a very small cone at the station and the diurnal hour of maximum thus gives the direction of anisotropy. It is found that during the active period of the solar cycle the diurnal hour of maximum passes through a cycle with an amplitude of two hours and when the solar activity wanes the direction of anisotropy for the nucleon component remains at 100° east of the sun-earth line. The diurnal hour of maximum for the neutron and meson components at Ottawa move from early hours in the beginning of the solar cycle (April 1954) to mid-afternoon hours in 1964 when the new minimum in solar activity is reached. Thus the direction of anisotropy is not fixed in space during a solar activity cycle.

10.9 ATMOSPHERIC PRESSURE COEFFICIENTS OF THE NUCLEON COMPONENT OF COSMIC RAYS DURING A SOLAR ACTIVITY CYCLE

Margaret D. Wilson and J. Katzman, National Research Council, Ottawa.

It is accepted that the energy spectrum of the cosmic ray intensity hardens during the active period of the solar cycle. This hardening may be reflected in a reduction in the value of the barometer coefficient. It will be shown that there is some evidence of this at high geomagnetic latitude stations such as Churchill (68.7°N) and Resolute (82.9°N). However, this variation is not so clear at Ottawa (56.8°N).

10.10 EXPERIMENTAL DETERMINATION OF THE ELECTRIC DIPOLE MOMENT OF CH*

D.H. Phelps, Department of Physics, University of British Columbia.

It is likely that the transition at 3400 mc/sec between the lambda doublets of the lowest rotational state of CH will soon be observed in interstellar space¹⁾. The strength of the microwave transition is proportional to the square of the electric dipole moment. An experimental value of the electric dipole moment obtained from Stark Effect on the electronic spectrum of CH will be presented.

* This work is supported by the National Research Council of Canada.

- 1) A.E. Douglas and G.A. Elliott, *Can. J. Phys.* 43, 496 (1965).

10.11 THE RELATIVE ABUNDANCE OF CARBON-12 TO CARBON-13 IN N-TYPE STARS
J.L. Climenhaga, Department of Physics, University of Victoria.

A comparison is made between computed and observed profiles of the (0,2)C₂ band at λ 6191, the (4,0)CN band at λ 6191 and the (2,0)CN band at λ 7850 in the spectra of several N-type stars. The observed profiles are from high-dispersion spectrograms taken at the Coudé focus of the 48" telescope of the Dominion Astrophysical Observatory. Features due to C¹³ are clearly present and in such strength as to indicate an abundance ratio C¹²/C¹³ between 4 and 20. Similar low values of this ratio have been found for several R-type stars in previous studies and are in agreement with values predicted by current theories of the synthesis of elements in stars.

Friday, June 11, 2:00 p.m.

Hebb 10

Session 11. THEORETICAL SYMPOSIUM

Chairman: F.A. Kaempffer

11.1 THE TRITON WAVE FUNCTION (30 min.)

Malcolm McMillan, University of British Columbia.

11.2 SEPARABLE NUCLEON-NUCLEON POTENTIALS (30 min.)

Frank Tabakin, Columbia University.

11.3 THE BETHE-SALPETER EQUATION BROUGHT TO TERMS (30 min.)

C. Schwartz, Berkeley.

11.4 PULSATING STARS (30 min.)

R.F. Christy, California Institute of Technology.

Friday, June 11, 2:00 p.m.

Hennings 201

Session 12. EXPERIMENTAL NUCLEAR PHYSICS II

Chairman: G.C. Neilson

12.1 ENERGY LEVELS IN Ir¹⁹³

N.M. Ahmed, P. Schmor, and M.W. Johns, McMaster University.

The currently accepted decay scheme of 31.5 hr. OS¹⁹³ is based almost completely on energy measurements determined by sodium iodide and magnetic spectrometers. An extensive series of γ - γ coincidence experiments has been carried out to establish the decay on a firmer footing. Lithium drifted germanium detectors have also been used to observe a number of new weak transitions. A decay scheme is proposed involving levels well established by energy and coincidence measurements at energies 0, 73, 139, 180, 278, 358, 362, 460, 558, 712 and 798 keV, and others established by either energy or coincidence measurements

at energies 620, 640, 657, 672, 698, 705, 737, 850, 876, 967 and 1047 keV. These account for 42 gamma ray transitions between the levels of Ir^{193} . (Levels previously established have been underlined).

12.2 THE DECAY OF Rb^{89}

J.E. Kitching and M.W. Johns, McMaster University.

15-minute Rb^{89} , daughter of 3.2-minute Kr^{89} , has been studied by sodium iodide and solid state spectrometers. The Krypton fission products from a sample of U^{233} irradiated beside the core of the McMaster reactor, were swept out to the laboratory area by a stream of helium gas, separated from other fission products by gas chromatography and trapped on carbon dust at liquid air temperature. The Rubidium daughters were collected on a charged foil. Samples of Rb^{87} , with about a 10% contamination from other Rubidium activities, were prepared by playing the "half-life game". The sodium iodide single and coincidence spectra were analysed by a non-linear least squares method using the 7040 computer. Energy levels established at 0, 1.035, 2.02, 2.281, 2.577, 2.73, 3.234, and 3.52 Mev permit the classification of twelve gamma ray transitions with intensities of greater than 2% per disintegration. Weaker transitions are difficult to disentangle from the background of other rubidium activities present.

12.3 STUDY OF THERMAL NEUTRON (n,α) REACTIONS IN THE RARE EARTH REGION

K. Beg, N.S. Oakey and R.D. Macfarlane, McMaster University.

A systematic study is being made of the thermal neutron induced (n,α) reaction throughout the periodic table. From a study of the alpha particle energy spectrum a knowledge of the spins and parities of the capturing states can be obtained. Cross section measurements yield data which can be compared with statistical model calculations of properties of highly excited states. We have made precise measurements of Q -values and cross sections of the n,α reaction for Sm^{147} , Sm^{149} and Nd^{143} targets. These results will be presented.

A technique for electrostatically focussing alpha particles in an intense neutron flux has been developed. This will be used in making high resolution measurements of the fine structure in the n,α process associated with transitions to excited states of the product nucleus. Details of this technique and its focussing properties will be discussed.

12.4 ELASTIC AND INELASTIC SCATTERING OF 14-MeV NEUTRONS FROM Ni AND Zr

R.L. Clarke and W.G. Cross, Chalk River Nuclear Laboratories.

Differential cross sections have been measured for elastic scattering of 14-MeV neutrons from Ni and Zr and for inelastic

scattering to their low-lying collective states. Elastic and inelastic groups were separated by time of flight, using the associated particle method previously employed¹⁾. The energy resolution at 14-MeV was 900 keV (FWHM), while the angular resolution was 5°. Targets were of natural isotopic composition. The optical model parameters derived from the elastic scattering results showed no significant differences from those of adjacent, non-closed-shell nuclei. For Ni, the inelastic measurements yielded an average quadrupole distortion parameter (β_2) of $0.23 \pm .02$ for the lowest 2^\pm states of Ni⁵⁸ and Ni⁶⁰, in agreement with values obtained by electromagnetic excitation. For Zr, we measured the angular distribution of a well-resolved peak, which corresponded to excitation of states between 2.1 and 2.8 MeV. No other inelastic peaks were observed.

1) R.L. Clarke and W.G. Cross, Nucl. Phys. 53, 177, (1963).

12.5 WEAK CROSS-OVER TRANSITIONS FROM THE 7.02- AND 4.97-MeV LEVELS IN Ne²⁰

T.K. Alexander, C. Broude, A.E. Litherland and R. Ollerhead, Chalk River Nuclear Laboratories.

Using the $C^{12}(C^{12}, \alpha\gamma)Ne^{20}$ reaction an enhanced E3 gamma-ray transition has been reported¹⁾ from the 5.63-MeV (3^-) state to the ground state (0^+) in Ne²⁰, and its relevance in the interpretation of the structure of the Ne²⁰ discussed¹⁾. Using the same reaction with improved sensitivity, we have obtained the intensities of the weak M2E3 transition from the 7.02 MeV (4^-) state to the 1.63-MeV (2^+) state and the M2 transition from the 4.97-MeV (2^-) state to the ground state. The 7.02-MeV level decays (60%) by E2 radiation to the 4.97-MeV state, which in turn decays almost entirely by E1 radiation through the 1.63-MeV state²⁾. Present measurements yield the intensity of the $7.02 \rightarrow 1.63$ transition to be 0.75% of this E1 transition. The intensity of the M2 transition from the 4.97-MeV state to the ground state is 0.5% of the branch to the 1.63-MeV state. The present measurements combined with lifetime measurements^{3,4)} give $|M|^2 \lesssim 6$ Wu (Weisskopf unit) for the enhancement of 4^- to 2^+ E3 transition from the 7.02-MeV state and $|M|^2 = 2$ mWu for the 2^- to 0^+ M2 transition from the 4.97-MeV state.

1) C. Broude, A.E. Litherland, and J.D. Pearson, Phys. Lett. 11, 321 (1964).

2) C. Broude, M.A. Clark and A.E. Litherland, Phys. Lett. 3, 118 (1962).

3) H.C. Evans, M.A. Eswaran, H.E. Gove, A.E. Litherland, and C. Broude, Can. J. Phys. 43, 82 (1965).

12.6 A SEARCH FOR A NEUTRAL π - π RESONANCE

T.F. Johnston, J.E. Pilcher, J.D. Prentice, and N.R. Steenberg, University of Toronto, L. Voyvodic, Argonne National Laboratory, and W.D. Walker, University of Wisconsin.

A study of π -p interactions, at 3.0 BeV/c laboratory momentum, is in progress. 20% of the two prong events present in 50,000 pictures of the MURA 30" hydrogen bubble chamber have been measured and analysed. In 70% of these, the final state particles have identified by kinematic fitting procedures. Correlations between the two pions in the $\pi^+\pi^-n$ final states may reveal the decay an I=0 resonance.

Events in which there are two or more neutral particles cannot be uniquely fitted by kinematics but the measurement of electron pairs from a lead and a tantalum plate, at the rear of the chamber, make possible the reconstruction of some events with two outgoing π^0 s. The neutral decay mode can thus be observed.

12.7 THE NUCLEAR SPIN OF Ag^{109m}

G.M. Stinson and R.G. Summers-Gill, McMaster University.

Atomic beam magnetic resonance techniques have been used to study Ag^{109m} . This 41-second isomeric state is the daughter of Pd^{109} produced by neutron irradiation of palladium metal. When that material is heated to about 1500°C a steady carrier-free beam of silver atoms is formed. The measured nuclear spin is 7/2 in agreement with the spin assignment obtained from half-life and conversion coefficient considerations. A continuation of the technique will allow the determination of the nuclear magnetic moment.

12.8 HIGH RESOLUTION STUDIES OF Mu-ATOMIC TRANSITIONS IN Au AND Pb*

C.K. Hargrove, National Research Council, E.P. Hincks, Carleton University, and H.L. Anderson and R.W. McKee, University of Chicago.

Studies previously reported¹⁾ of the radiations from muonic atoms with a lithium-drift germanium diode have been supplemented by further measurements using high-Z targets. We report here some results obtained with Pb^{206} , natural Pb and Au. As before, the muons (10^4 stops per sec) were from the Chicago synchrocyclotron muon channel, but a larger (4.4 cm^3) diode²⁾ was used and the Maniac III computer facilitated on line data-handling. Transitions from states with $n = 6$ are observed. Isotope shift is seen in the Pb $2p - 1s$ transitions; these are more energetic for Pb^{206} than for Pb^{208} but not by as much as the 16 KeV expected for an $A^{1/3}$ nuclear radius dependence. For Au the $2p_{3/2} - 1s$ line exhibits pronounced hyperfine splitting. Individual components are not resolved but the complex structure is explained moderately well by electric quadrupole interaction

between the $2p_{3/2}$ state and the nuclear ground state. The significant deviations may be due to dynamic effects.

* Work supported, in part, by the U.S. Office of Naval Research.

- 1) H.L. Anderson et al. Proceedings of the International Conf. on High Energy Physics, Dubna, Aug. 1964. To be published.
- 2) Kindly loaned to us by Atomic Energy of Canada Ltd., Chalk River Nuclear Laboratories.

12.9 LEVELS IN Pb^{207}

C.R. Cothorn and R.D. Connor, University of Manitoba.

The beta decay of Tl^{207} and the alpha decay of Po^{211} were investigated as part of a study of the properties of the active deposit of actinium. The active deposit consists of Pb^{211} and its daughter products (Bi^{211} , Po^{211} , Tl^{207} and Pb^{207}). The beta decay of Tl^{207} involved a 1.431 Mev (99.55%) feed to the ground state and a 0.531 Mev (0.45%) feed to the 900 keV excited state in Pb^{207} . An upper limit of 0.01% was placed on a possible feed to the 560 keV level and an upper limit of 0.002% was placed on the possible existence of a feed to a 1100 keV level in Pb^{207} . Separated sources of Tl^{207} were prepared by electrostatically collecting the recoil product of the Bi^{211} alpha decay. The gamma ray spectrum of these Tl^{207} sources revealed one gamma ray at 900 ± 7 keV. The alpha decay of Po^{211} involved a 7.455 Mev (99.4%) feed to the ground state and a 6.90 Mev (0.4%) feed to the 560 keV level in Pb^{207} . An upper limit of 0.2% was placed on a possible feed to the 900 keV level in Pb^{207} .

12.10 MEASUREMENT OF LM/K ELECTRON CAPTURE IN Sn^{113} AND Cd^{109} AND THE K/(L+M) INTERNAL CONVERSION OF In^{113*} AND Ag^{109*} TRANSITIONS WITH A SOLID STATE DETECTOR[†]

D. Etti, D.R. Brundrit^{††} and S.K. Sen, Allen Physics Laboratory, University of Manitoba, Winnipeg-19.

A coincidence method¹⁾ using a solid state detector has been employed to yield the K-electron to total electron capture ratios which are independent of fluorescence yield, x-ray detection efficiency and absorption of x-rays in the source and in the detector shielding material. The ratio, P_{LM}/P_K , of electron capture from higher shells to that from the K-shell has been determined to be 0.16 ± 0.02 for Sn^{113} and 0.90 ± 0.20 for Cd^{109} giving electron-capture decay energies of $280^{+XX} keV$ and $41 \pm 3 keV$ respectively. The K/(L+M) conversion coefficients of the 393 keV transition of In^{113*} and the 88 keV transition of Ag^{109*} have been measured to be 4.5 ± 0.1 and 0.83 ± 0.02 respectively.

† Work supported by the National Research Council of Canada.

†† Present address: Shell Oil Company of Canada, Edmonton.

- 1) D.R. Brundrit and S.K. Sen, Nuclear Physics (1965), (in press).

Session 13. ATOMIC AND MOLECULAR PHYSICS

Chairman: A.M. Crooker

13.1 ROTATIONAL STRUCTURE AND AUTO IONIZATION LEVELS IN THE PRODUCTION OF H_2^+

D.J. Keenan, E.M. Clarke, and A. Weingartshofer, Saint Francis Xavier University.

Data for the formation of H_2^+ by electron impact have been analyzed with the help of a digital computer. The second derivative of the data has proved to be the most useful form of representation. The very reproducible structure obtained has been correlated with rotational and autoionizational levels as well as with the vibrational levels.

13.2 CALCULATION OF THE VIBRATIONAL FREQUENCY PERTURBATION IN COMPRESSED GASEOUS AND SOLID HYDROGEN

A.D. May and J.D. Poll, Department of Physics, University of Toronto.

If the frequency perturbation of compressed hydrogen is expressed as a power series in the density it is possible, with the aid of a statistical theory, to extract from the experimental values for the linear term at different temperatures the separate contributions arising from the overlap and dispersion forces. The theoretical value of the contribution calculated from the well known London dispersion forces agrees with the experimental value. If the experimental values for the overlap and dispersion force contributions to the shift (terms linear in the density) are used to calculate either the term quadratic in the density or the shift in frequency for solid hydrogen the agreement with measured values is satisfactory provided non-additivity of inter-molecular forces is considered in the first case and the zero point motion of the lattice is considered in the second case.

13.3 THE INFRARED ABSORPTION SPECTRUM OF SOLID DEUTERIUM AND SOLID HYDROGEN DEUTERIDE

A.Crane and H.P. Gush, Department of Physics, University of Toronto.

The induced rotation-vibration absorption spectrum of the isotopes of hydrogen have been measured at a temperature of 1.9°K. The fundamental band of solid D_2 closely resembles that of solid H_2 which has been previously investigated.¹⁾ The spectrum of solid HD however shows several unusual features, one of which is the appearance of a $\Delta J = 1$ transition, forbidden in H_2 and D_2 . The induced spectra of the solid hydrogens show phonon branches accompanying molecular transitions. The phonon spectrum of solid HD is however much different from that of H_2 and D_2 ; it appears that there is a strong interaction between

the rotation of the molecule and its translational motion in the lattice.

1) Gush, Hare, Allin, and Welsh, Can. J. Phys. 38, 176 (1959).

13.4 PRESSURE-INDUCED INFRARED ABSORPTION OF D_2 AND D_2 -FOREIGN GAS MIXTURES AT ROOM TEMPERATURE.

S.T. Fai, S. Paddi Reddy, and C.W. Cho, Memorial University of Newfoundland.

The fundamental vibration-rotation absorption band of deuterium, induced by inter-molecular forces, has been studied in pure D_2 and D_2 -foreign gas mixtures at pressures up to 1500 atm. The splitting of Q-branch into two components, Q_P and Q_R has been observed in the absorption contours of pure D_2 as well as in D_2 -foreign gas mixtures. The pronounced S(0) and S(2) components with an indication of the S(1) and O(2) components were observed in pure D_2 spectrum, and these became more prominent with an indication of other components in D_2 -A mixtures. The binary absorption coefficients obtained in the present investigation will also be discussed.

13.5 ITERATION AND ITERATION-VARIATION METHODS FOR LOW ENERGY ELECTRON-ATOM COLLISION PROBLEMS*

M. Kraidy[†] and P.A. Fraser, Department of Physics, University of Western Ontario.

The coupled integro-differential equations that arise in the eigen-function expansion approach to low-energy electron-atom collisions have been solved by iterative methods, variational methods, and by iteration-variation methods. One iterative method is that of McEachran and Fraser which is based on an integral equation formulation of the equations with a certain asymptotic form for the solutions. There are cases for which this method does not converge or converges very slowly.

We present here an alternative iterative method, also based on the integral equation formulation, but with different asymptotic form for the solutions. This method generally gives convergence where the other fails and often gives convergence in fewer iterations.

We also present a one-parameter iteration-variational method in which the trial functions used in the Kohn variational principle are expressed as a linear combination of two iterated solutions from either of the iteration methods.

* This work was supported by the National Research Council of Canada.

† Holder of a National Research Council Studentship.

13.6 SENSITIZED FLUORESCENCE IN POTASSIUM INDUCED BY COLLISIONS WITH NEON AND KRYPTON ATOMS*

G.D. Chapman[†] and L. Krause, Department of Physics, University of Windsor.

The transfer of excitation between the $4^2P_{1/2}$ and $4^2P_{3/2}$ resonance levels in potassium was investigated by studying sensitized fluorescence in potassium vapor - inert gas systems. The fluorescence was excited by means of one component of the potassium resonance doublet and the relative intensities of both components present in fluorescence, were measured over a range of inert gas pressures. Measurements at exceedingly low light intensities were made possible by using very efficient light sources and fluorescence tubes, recently developed in this laboratory. The inelastic collision cross sections for K - Ne collisions are $Q_1(4^2P_{1/2} \rightarrow 4^2P_{3/2}) = 1.1 \times 10^{-15} \text{ cm}^2$ and $Q_2(4^2P_{1/2} + 4^2P_{3/2}) = 0.7 \times 10^{-15} \text{ cm}^2$. The values for K - Kr collisions are $Q_1 = 3.3 \times 10^{-15} \text{ cm}^2$ and $Q_2 = 2.1 \times 10^{-15} \text{ cm}^2$. In both cases the ratio Q_1/Q_2 agrees with the value predicted from the principle of detailed balancing.

* Research supported by National Research Council.

† Holder of an N.R.C. studentship.

13.7 THE MEASUREMENT OF RELATIVE OSCILLATOR STRENGTHS IN NEON

A.M. Robinson and R.A. Nodwell, Department of Physics, University of British Columbia.

The relative oscillator strengths of transitions between the two lowest excited states of neon have been measured. The method used employs an intensity-modulated background neon source and a photomultiplier coupled with a lock-in-amplifier for detection. The absorption tube is a low-pressure multi-electrode dc discharge tube, which enables 6 different discharge lengths to be used. A comparison of the theoretical and experimental curves of transmission versus discharge length allows the emission-to-absorption line width ratios and the relative oscillator strengths for lines with a common lower level to be determined. This determination of the relative strengths assumes that the density distribution is a function of the radial distance from the centre of the tube only. The relative density distribution of the atoms in the lower level of the transitions has been determined as a function of radius.

13.8 RADIATIVE LIFETIMES OF EXCITED NEON

H.W.H. Van Andel and R.A. Nodwell, Department of Physics, University of British Columbia.

Radiative lifetimes of excited states in Neon are being measured directly using time resolved spectroscopic methods. The light decay from a light source produced by a pulsed electron

beam is measured as a function of time for several transitions in Neon. The rates of decay together with the relative line strengths of the transitions give an absolute measurement of transition probabilities.

13.9 REVERSAL TEMPERATURES IN EXCITED NEON

J.C. Irwin and R.A. Nodwell, Department of Physics, University of British Columbia.

The relative population densities of the 2S and 2p levels in Neon are measured by a reversal temperature technique¹⁾. If these measurements are combined with the results of relative emission line intensities one obtains values for the relative transition probabilities. The measurements are made at currents low enough to ensure negligible self absorption. An estimate of the amount of self absorption is made by total absorption measurements at the lines concerned.

1) Nodwell and Irwin, Canadian Journal of Physics (to be published).

13.10 COHERENCE PROPERTIES OF CROSS-CORRELATED MODES I

Roscoe C. Williams, Department of Physics, University of British Columbia.

The Coherence of a Fabry-Perot mode is determined by the ability of that mode to interfere with itself, which according to definition^{1,2)} is related to the Auto-correlation function of stationary fields.

This concept is extended to include the ability of two different modes to interfere with each other when electrons, which are radiating into these modes, are coupled by some interaction. The modes are then cross-correlated, and now possess both auto and cross-correlation functions.

These functions are calculated using the Action Principle of Julian Schwinger³⁾, which yields coupled equations of motion for the amplitudes of the field oscillators.

These are solved using Schwinger's Thermodynamic Green's functions. A set of coupled equations results for the Advanced and Retarded Green's functions, which are solved by a combination of Fourier Transform and Matrix methods.

The Green's functions are used to calculate the auto- and cross-correlation functions, for a Fabry-Perot Cavity filled with a lasing Two-level Medium. The losses in the medium, the finite line width of the upper level along with the driving current are taken into account.

1) L. Mandel and E. Wolf, J. Opt. Soc. Am. 51, 815 (1961).

2) R.J. Glauber, Phys. Rev. 130, 2529 (1963).

3) Julian Schwinger, J. Math. Phys. 2, 407 (1961).

13.11 COHERENCE PROPERTIES OF CROSS-CORRELATED MODES II

Roscoe C. Williams, Department of Physics, University of British Columbia.

The Auto and Cross-correlation functions obtained by the methods outlined¹⁾ in (I) are discussed from the point of view of experiment.

The Auto-Correlation function for each mode can be measured by the two detector coincidence counting technique of Hanbury, Brown and Twiss²⁾. The cross-correlation for these modes is the coincidence counting rate between any two of the four detectors used for the auto-correlation. They must not be the same two used for a given auto-correlation.

The Fourier transforms of these counting rates (correlation functions) shows that the experiment should reveal five lines. Each mode contains a coherent and incoherent part, the latter being intimately connected to the former. The fifth line consists of the spontaneous emission.

The correlations of the atomic currents due to the transitions made by the electrons between the laser levels determines the coherence time of all lines except the spontaneous emission. The amplitudes of all the lines are dependent on these correlations. Comparison of the experimental and theoretical Fourier transformed distribution functions determines these auto and cross-atomic current correlations.

- 1) Roscoe C. Williams, Coherence Properties of Cross-Correlated Modes I (preceding abstract).
- 2) R. Hanbury Brown and R.Q. Twiss, Proc. Roy. Soc. (London) A243, 291 (1958).

13.12 DETERMINATION OF DECAY RATES OF NON-RADIATIVE TRANSITIONS

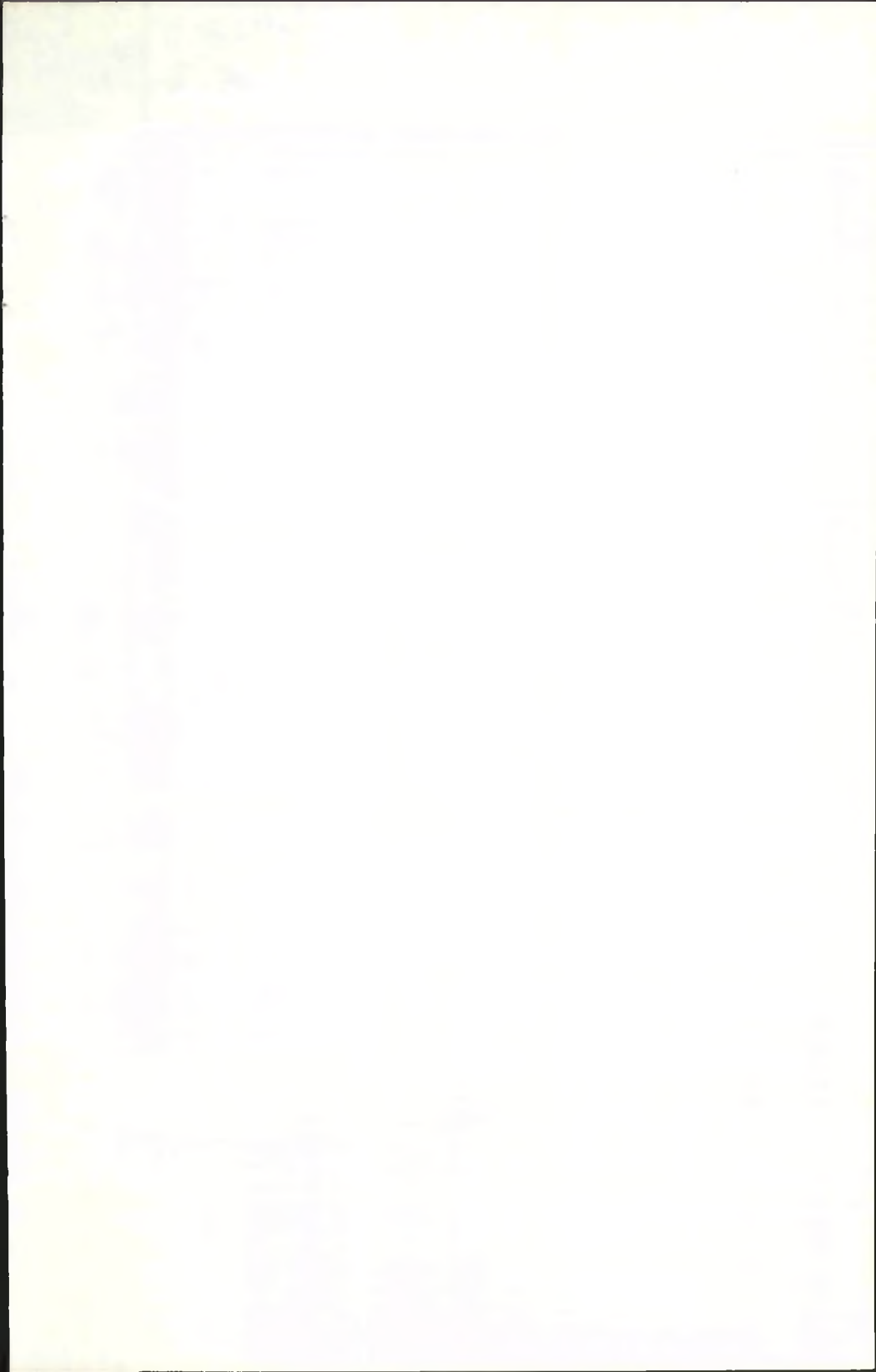
Roscoe C. Williams, Department of Physics, University of British Columbia.

A large number of solid optical laser materials possess large pump-bands that are connected to meta stable (lasing) levels by non-radiative decay rates.

These decay rates as yet have not been determined theoretically. An experimental method of measuring these decay rates is proposed based on the results^{1,2)} that a laser level will split if the pump-rate is high enough. The splitting is given by the square root of the sum of the squares of the pump-rate and phonon transition rate (non-radiative decay rate).

Measurement of both pump-rate and splitting will yield the non-radiative decay rate.

The splitting can be measured by optical super heterodyne techniques.



magnetic field (B_u) is:

$$B_u(r) = B_p(r) + K_1 C(r-x) J(x)$$

where, $C(r-x) = \pm (1 - (1 + \rho^2 / (r-x)^2)^{-1/2}) (1 + (r-x)^4 / \rho^4)^{-1/2}$

K_1 is a constant

ρ is the radius of the tube containing the probe

and, $C(r-x)$ is positive if r is greater than x .

Assuming that the discharge can be represented by a set of coaxial current sheets of varying current density, the unperturbed magnetic field (B_u) can be deduced from the perturbed magnetic field (B_p) and the correction factor (C).

$$(B_u)_r = (B_p)_r + K_2 C_{rx} D_{xx} (B_u)_x$$

or
$$(B_u)_x = (\delta_{rx} - K_2 C_{rx} D_{xx})^{-1} (B_p)_r$$

where, D_{xx} is a matrix involving the differential operator

and K_2 is a constant.

Using the calculated unperturbed magnetic field (B_u), the current density distributions are determined for several initial pressures of Argon in the Z-pinch.

15.3 TEMPERATURE AND VELOCITY IN A PLASMA JET*

B. Ahlborn, Department of Physics, University of British Columbia.

Temperature and velocity in a subsonic plasma jet operated with argon have been measured with spectroscopic and optic methods. These values have been compared with predictions from a simple two-step model, which is based on the equations of conservation of mass, momentum and energy. Measurements and calculation agree within 15%.

* This work was carried out in the Institut für Plasmaphysik Garching bei München.

15.4 SCATTERING OF LASER BEAM FROM A θ -PINCH PLASMA

P.W. Chan and R.A. Nodwell, Department of Physics, University of British Columbia.

Light from a giant pulse ruby Laser is used to demonstrate scattering by a θ -pinch plasma. The scattered radiation is observed at right angles to the incident beam, using a monochromator and a photomultiplier. Special precautions are taken to cut down the stray light of the laser entering into the detector. The incident laser beam is focused at a point near the centre of the pinch, and measurements are made at a time corresponding to the seventh compression of the plasma. Results show that the scattered radiation has a Gaussian profile with a half width of 65 Å, corresponding to an electron temperature of 5 eV. Detailed numerical calculations show that the experimental points are best fitted by a value of α equal to 0.5

where α is the ratio of scale length for scattering to the Debye length. From the value of α the electron density n_e is deduced to be $1.1 \times 10^{16} \text{ cm}^{-3}$.

15.5 ELECTRON TEMPERATURE MEASUREMENTS BASED ON THE DIAMAGNETIC PROPERTY OF A PLASMA

S.Q. Mah and H.M. Skarsgard, University of Saskatchewan, Saskatoon.

Electron temperature measurements have been carried out in a low-pressure rf discharge in the presence of a magnetic field by making use of the diamagnetic property of a plasma. The diamagnetic signal induced in a coil wound around the plasma container is observed during the pulsed discharge. Integration of this signal, together with an independent determination of the electron concentration, gives the electron temperature in the discharge. Measurements in argon at pressures from 0.5 to 26 microns give electron temperatures from approximately 10^4 to 10^4 °K. The duration of the diamagnetic signal corresponding to breakdown is a minimum at a pressure of 3 microns. This can be explained by noting that at this pressure the rf radian frequency is approximately equal to the electron collision frequency so that the electrons receive the maximum power from the rf electric field.

15.6 AN EXPERIMENTAL INVESTIGATION OF EQUILIBRIUM CONDITIONS IN A SHOCK PLASMA

C.R. Neufeld, H.G. James, and A.J. Barnard, Department of Physics, University of British Columbia.

Photo-electric measurements were made of the shock-excited spectra of argon-helium and argon-oxygen mixtures. The electron densities and the temperatures of the plasma components behind the shock wave were deduced from the spectroscopic measurements, assuming thermal equilibrium. For each mixture the temperatures of the two components were in fairly good agreement, supporting the thermal equilibrium assumption. On the other hand, the temperatures and electron densities differed significantly from the values expected for a one-dimensional shock wave.

15.7 RADIATIVE DECAY RATES IN HYDROGEN PLASMAS

A.J. Barnard and J.H. Williamson, Department of Physics, University of British Columbia.

The rate of decay of excitation by emission of resonance radiation has been computed for hydrogen plasmas, taking into account the imprisonment of the radiation. For dense laboratory plasmas the resonance radiation escapes fairly readily, due to the large Stark broadening of the resonance lines. For these plasmas the effective radiative decay rate is of the same order as the collision decay rate (10^6 sec^{-1}).

Session 16. THEORETICAL TOPICS

Chairman: E.M. Henley

16.1 A THEORY OF BETA RAY ATTENUATION

W.G. Cross and S.A. Kushneriuk, Chalk River Nuclear Laboratories, Chalk River.

The one-group Boltzmann equation has been applied to the problem of attenuation of a beta spectrum as a whole. We attempted to obtain an analytical solution without assuming the angular distribution or making the usual, incorrect assumptions that single scattering is nearly isotropic or that absorption is unimportant compared to scattering. The equation was solved in one dimension (plane source of infinite area) with only the approximations of predominantly small-angle scattering and that the ratio of absorption and transport cross sections is independent of distance from the source. With these assumptions the Boltzmann equation reduced to a separable partial differential equation in distance and angle. The distance equation was elementary. The angle equation was a new eigenvalue equation for which eigenfunctions and eigenvalues were calculated numerically. It is noteworthy that the asymptotic variation of the spherical flux so obtained is very similar to those given by the P_1 spherical harmonic approximation and by diffusion theory. However, the present solution also gives the angular distribution and the variation of flux close to the source. This variation agrees with that measured for Tl^{204} beta rays. In the comparison, the transport cross section was determined empirically by matching the attenuation at large distances.

16.2 AMPLITUDES FOR SCATTERING VIA SEPARABLE NONLOCAL POTENTIALS

Ronald Davis and Malcolm McMillan, Department of Physics, University of British Columbia.

An exact, closed form¹⁾ for the partial wave amplitude for nonrelativistic scattering via a class of separable, nonlocal potentials is given, and its analytic properties are investigated in detail. Restrictions are placed on the potential to permit a Sommerfeld-Watson transformation, and a double dispersion relation for the total scattering amplitude is obtained. Convergence of the spectral integrals is discussed.

1) M. McMillan, *Nuovo Cimento* 29, 1043 (1963).

16.3 LOW TEMPERATURE BEHAVIOUR OF FINITE BOSE-EINSTEIN ASSEMBLIES

D.F. Goble and L.E.H. Trainor, University of Toronto.

Osborne has shown that, while an ideal two-dimensional Bose gas does not undergo Einstein condensation, such a system does exhibit abrupt accumulation into the lowest state at a temperature below the condensation temperature of the bulk gas.

The accumulation temperature goes to zero, however, as the number of particles is increased without limit. Observing that an ideal Bose assembly of any finite thickness behaves as if it were two-dimensional, Ziman¹⁾ drew a comparison between the variation of the accumulation temperature with thickness in such a system and the variation of the lambda transition temperature with thickness in actual helium films. He concluded that, in so far as the lambda transition is related to the low temperature behaviour of an ideal Bose gas, bulk helium must be regarded as made up of a collection of "maximal finite assemblies".

We have carried out a numerical study of such assemblies on the University of Toronto 7090 computer to determine their thermodynamic properties and the dependence of these properties on assembly size, particle density and assumed boundary conditions. The relevance of these results to the problem of liquid helium will be discussed.

1) J.M. Ziman, Phil. Mag. 44, 548 (1953).

16.4 SHELL MODEL CALCULATION ON OXYGEN-18 WITH A VELOCITY-DEPENDENT RESIDUAL INTERACTION

J.M. Pearson, Université de Montréal.

Shell model calculations of the positive parity levels of O^{18} have been performed with a view to testing the hypothesis that the residual inter-nucleon interaction can be taken as the free nucleon-nucleon interaction. Our interaction potential, of necessity velocity-dependent, is of a form which has been shown¹⁾ to be favorable to the saturation of nuclear matter, unlike the potential of Green²⁾, and has been fitted³⁾ with precision to the two-nucleon data. We compare the results with those of a similar calculation⁴⁾ which used Green's potential.

1) R.K. Bhaduri and M.A. Preston, Can. Journ. Phys. 42, 696 (1964).

2) A.M. Green, Nuc. Phys. 33, 218 (1962) and Phys. Lett. 3, 60 (1962).

3) F. Trudeau, M.Sc. thesis, Université de Montréal (1965).

4) B.H.J. McKellar, Phys. Rev. 134, B1190 (1964).

16.5 THE INVERSE PROBLEM OF PARTICLE MOTION

P.S. Naidu and K.O. Westphal, Department of Geophysics, University of British Columbia, and Bedford Institute of Oceanography.

In the usual problem of particle motion in an electrostatic field, the potential distribution is given and the particle trajectory is sought. In the development of an efficient ion source for a mass spectrometer, the inverse problem arises, that is, for a prescribed path of a particle, the potential distribution is sought such that the particle follows the prescribed path.

In this connection, we have established the following two theorems:

- 1) There exists a potential distribution to guide a particle along any prescribed path.
- 2) A group of particles (non colloidng) may be guided along any prescribed set of paraxial paths.

Applying the theory, two types of ion optical systems are proposed; stability analysis, however, shows that only one of them is stable.

16.6 LOW ENERGY CAPTURE CROSS/SECTIONS FOR $D(p\gamma)He^3$

D.H. Rendell, Memorial University of Newfoundland.

Numerical calculations have been made of the capture cross-sections of $l = 0$ and $l = 1$ protons in the 1 MeV energy range. Using Coulomb state functions for the unbound states and exponential-type state functions for the bound states estimates have been made of the contribution to the cross-section of the various symmetry states of He^- . Reasonable agreement with experimental results have been obtained.

16.7 THE GEOMETRICAL APPEARANCE OF LARGE OBJECTS MOVING AT RELATIVISTIC SPEEDS

G.D. Scott and M.R. Viner, Department of Physics, University of Toronto.

The calculated geometrical appearance of objects¹⁾ subtending large angles at the observer and moving at relativistic speeds is illustrated by diagrams of a plane grid and perspective views of a group of boxes. The distortions in appearance result from varying change of scale in the direction of motion and the hyperbolic shape of planes perpendicular to the motion. Contrary to an impression which might be conveyed by some papers²⁾ on the subject, the Lorentz contraction is visible under suitable conditions, in particular for observations approximately at right angles to the motion.

1) H.A. Atwater, J. Opt. Soc. Am. 52, 184 (1962).

2) J. Terrel, Phys. Rev. 116, 1041 (1959).

16.8 A PECULIAR PROPERTY OF THE FERMI-YANG EQUATION

B.C. McInnis and T.F. Morris, McGill University, Montreal.

As part of a survey of methods and models for dealing with relativistic bound state problems, the structure of the Fermi-Yang equation for pions was investigated. This equation possesses a peculiar defect which thus far has been masked by the use of a square well potential. If a continuous potential such as a Yukawa potential is used, it is shown that the binding energy of the nucleon-antinucleon pair cannot be comparable to or greater than a nucleon mass.

16.9 A STUDY OF THE RENNER EFFECT IN THE LINEAR XY_2 MOLECULE

Cosmo Carlone, Department of Physics, University of British Columbia.

In linear molecules, the Renner effect is the splitting of the degenerate electronic levels by those nuclear vibrations which break the symmetry of the nuclear field.

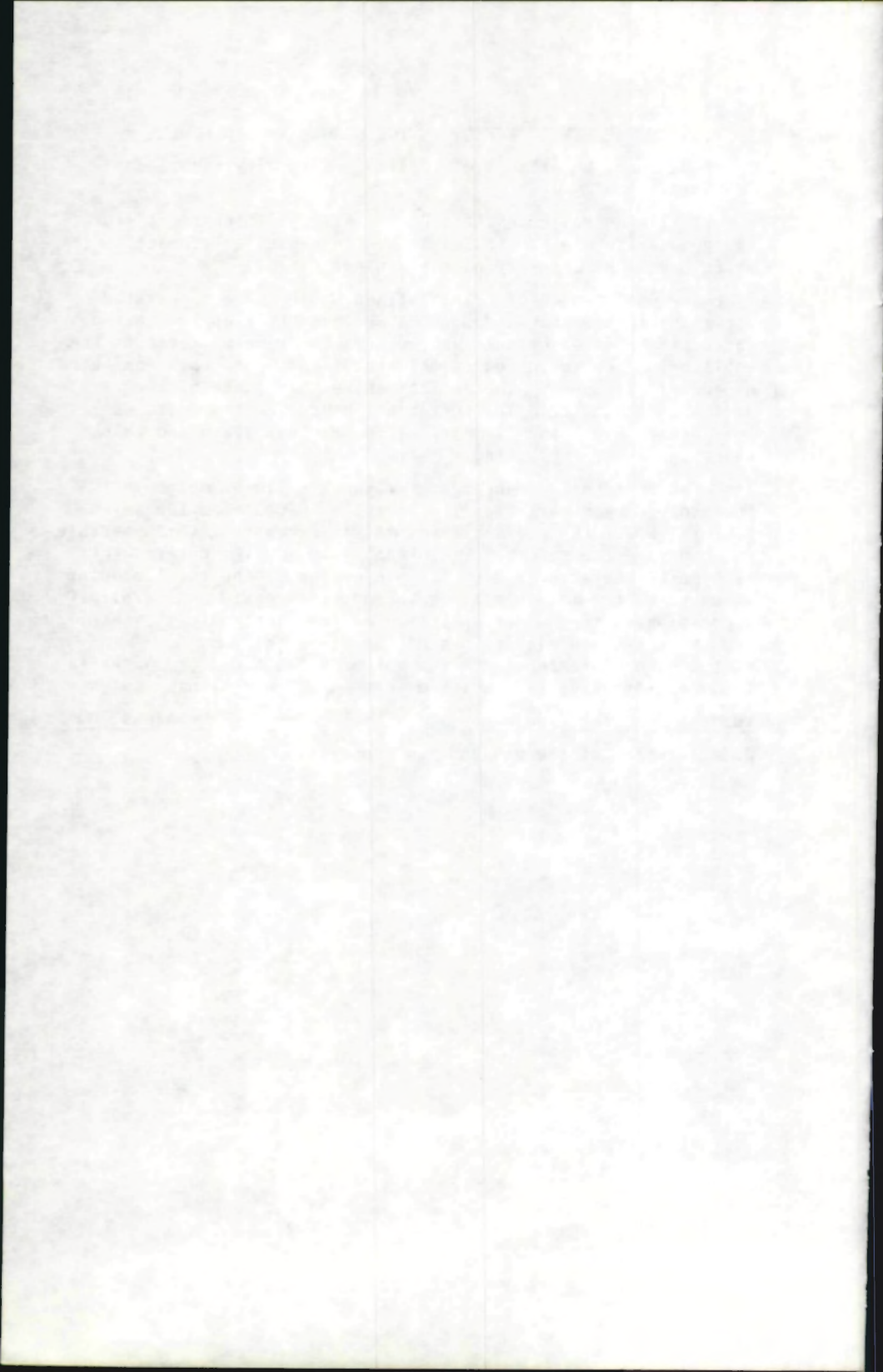
The Hamiltonian of the XY_2 linear molecule is separated according to the static approximation. In this approximation, the unperturbed electronic states have the same symmetry as the equilibrium configuration of the nuclei and hence their azimuthal dependence is known. The nuclear states are those of the simple harmonic oscillator. The perturbation Hamiltonian contains terms which break the symmetry of the nuclear field and which cause the Renner splitting.

The Schroedinger equation for the XY_2 linear molecule is then solved by a variational principle. Because of the selection rules for the non-vanishing matrix elements, it is possible to subdivide the secular determinant into smaller determinants each being characterized by the projection of the total angular momentum of the molecule along the molecular axis. An explicit expression of the Renner splitting of the electronic Π state, and the corrected eigenvalues of the electronic Σ , Π , Δ states with vibrational quantum number $v = 0$ and 1 are given in terms of six quantities which depend on the electronic states.

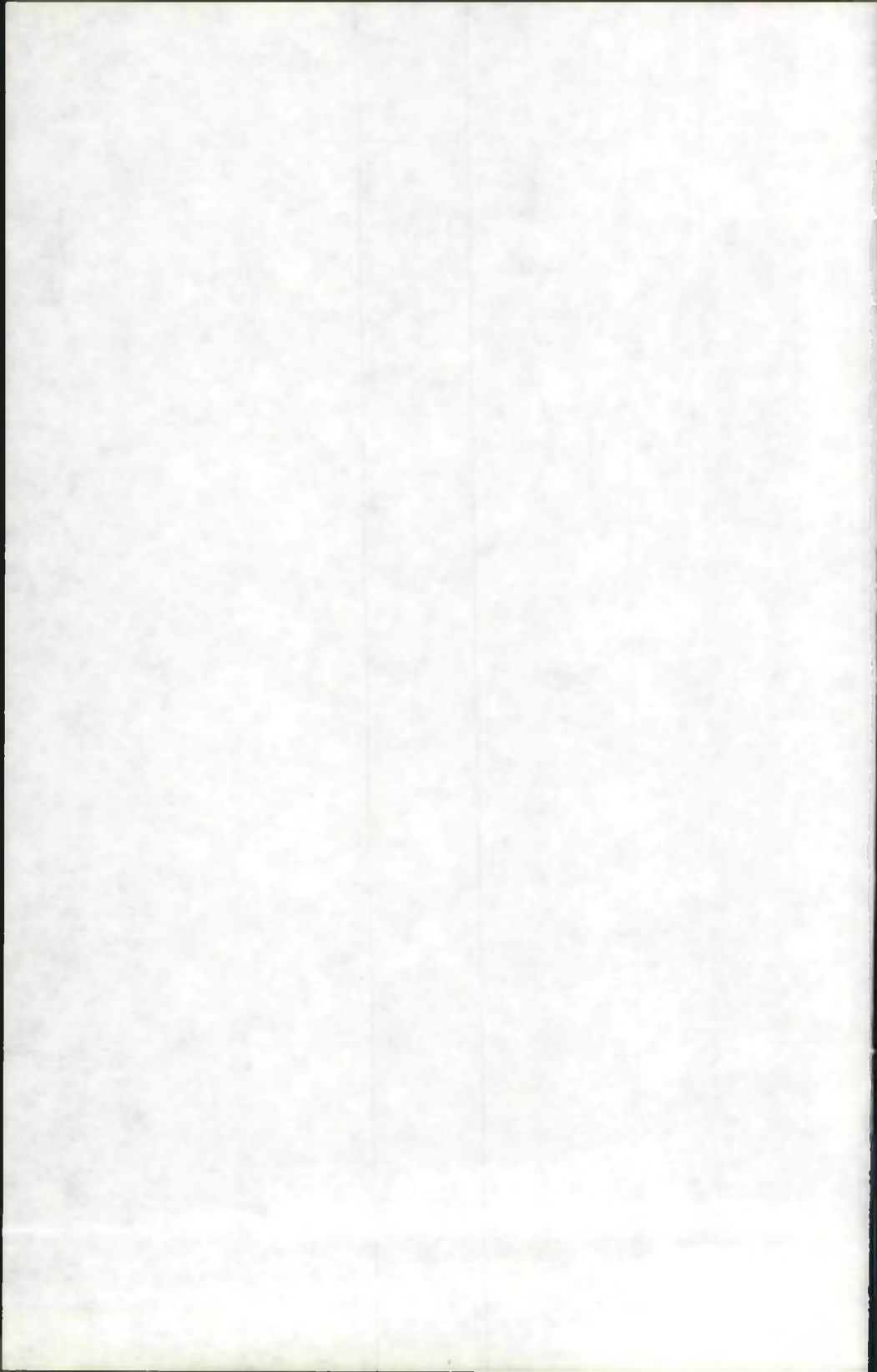
Saturday, June 12, 2:00 p.m.

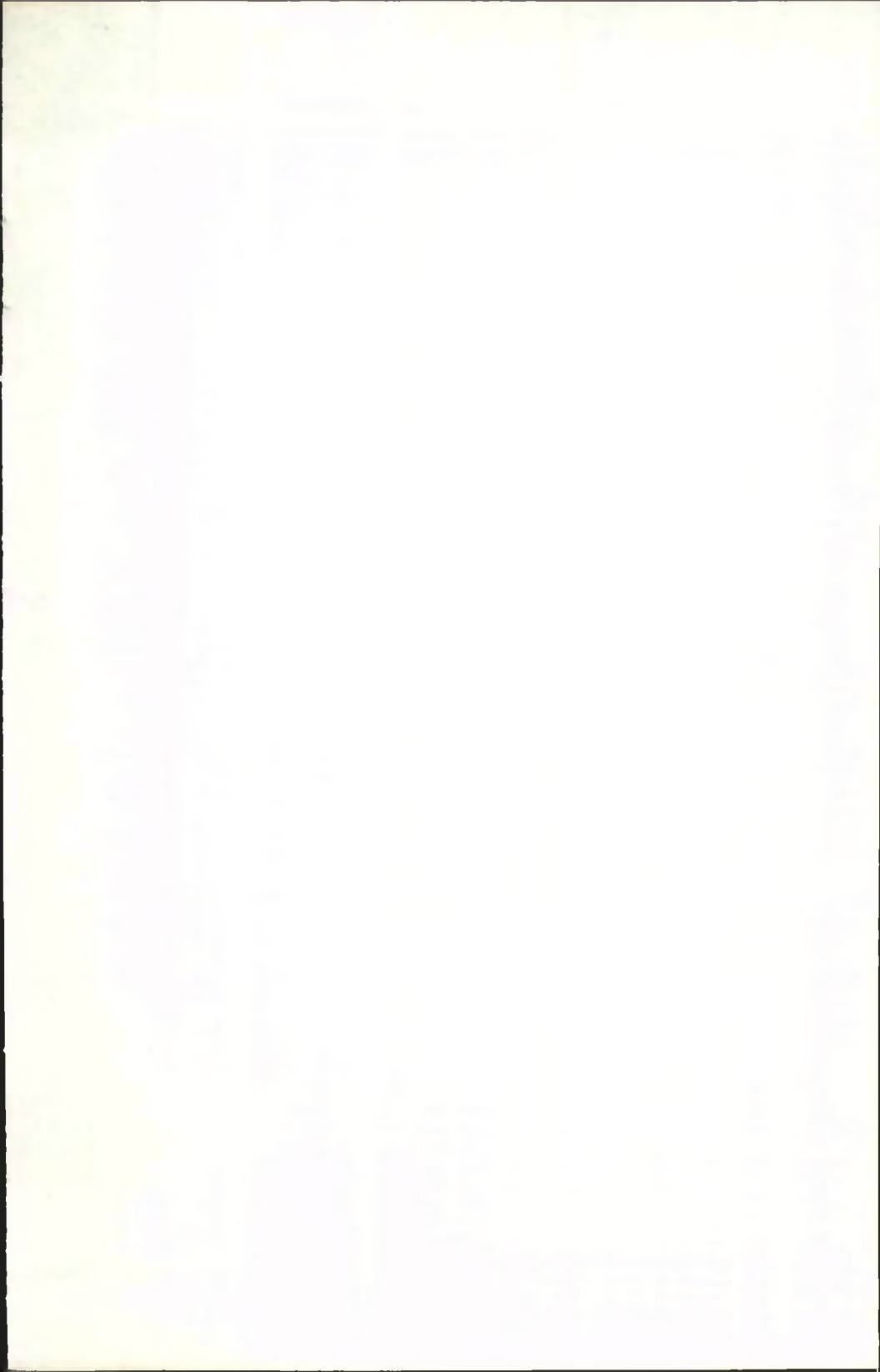
Hennings 303

Joint meeting of the old and new Councils.









LITHOGRAPHED BY:
(Exclusive of Cover)

BEST-PRINTER CO. LTD.
VANCOUVER, B.C.

ABOUT THE ASSOCIATION

The Canadian Association of Physicists invites applications for membership from physicists, scientists and engineers whose work is related to physics, from teachers of physics, and from university students studying physics or an allied course. Canadian citizenship or residence in Canada is not a requirement.

The objects of the Association, as set forth in the Constitution and By-Laws (Revised 1956) are:

- (a) to further the advance of the Science of Physics;
- (b) to promote the use of physical discoveries in the interest of mankind;
- (c) to promote knowledge in the Physical sciences and dissemination of information relating thereto in and between all sections and regions of Canada;
- (d) to advance mutual understanding and co-operation between physicists, on the one hand, and universities, research organizations, and industry, on the other.

Since its inception in 1945 the Association has grown steadily in size and vitality. Today we have a total membership of 1,507 (658 full members, 409 associates, 431 students). The activities of the Association are many and varied. Each year the C.A.P. Medal is awarded to an outstanding Canadian physicist. The C.A.P. Prize is presented annually to the most promising Honours Physics graduate from a Canadian university. Lectures designed to give undergraduates a close-up view of physics at other universities are sponsored. This year five different lecturers visited universities and colleges from coast-to-coast. The annual C.A.P. Congress is a three-day meeting of the society at which invited and contributed papers and symposia afford the opportunity for discussion of topics of current interest. A nationwide high school competition is carried out. The Association publication *Physics in Canada* contains articles of topical interest, news of physics and physicists in Canada, book reviews, etc. In this issue, abstracts of the Annual Congress are published.

Membership is available in four grades—full member, associate member, student member and corporate member. All members receive the Association's own bulletin, *Physics in Canada*, and membership lists from time to time. Arrangements have been made so that members may subscribe to various journals at reduced cost. During 1965, these include: *Canadian Journal of Earth Sciences*, *Canadian Journal of Physics*, *Contemporary Physics*, and *The Physics Teacher*. The annual membership fees of the Association are as follows: Full members \$13.00; Associate members, \$6.00; Student members, \$2.00.

Subject Divisions of Theoretical Physics, Earth Physics and Medical Physics are active. When the demand warrants, other divisions may be formed.

For further details regarding membership or the Association write the Registrar, Canadian Association of Physicists, McMaster University, Hamilton, Ontario, or see the nearest Council member.

CORPORATE MEMBERSHIP

The constitution of the Association provides for the enrollment of Corporate Members. Corporate Membership is open to all corporations, firms, institutions or individuals who wish to contribute to the Educational Trust Fund of the Association. This fund is being put to good use in furthering the educational activities of the Association—in particular the C.A.P. Secondary School Prize examination which has been operating with such success. Arrangements for corporate membership should be made by contacting Dr. R. H. Hay, Aluminum Company of Canada, Kingston, Ontario.

We take pleasure in welcoming the following corporate members enrolled since the last Congress:

D. VAN NOSTRAND CO.;
POLYMER CORP. LTD., SARNIA;
THE STEEL COMPANY OF CANADA, LTD., HAMILTON;
DOMINION FOUNDRY AND STEEL;
DE HAVILLAND AIRCRAFT;
DOMINION ELECTROHOME;
CANADIAN WESTINGHOUSE;
R.C.A. VICTOR CO. LTD.;
BRITISH-AMERICAN OIL CO. LTD.;
NORTHERN ELECTRIC CO. LTD.;
COMPUTING DEVICES OF CANADA;
ALLAN CRAWFORD ASSOCIATES LTD.;
THE MACMILLAN COMPANY OF CANADA LTD.
ABREX SPECIALTY COATINGS LTD., OAKVILLE